Cosmic Star Formation, Reionization, and Constraints on Global Chemical Evolution

Article *in* The Astrophysical Journal · May 2004

DOI: 10.1086/425649 · Source: arXiv

Cosmic Star Formation, Reionization, and Constraints on Global Chemical Evolution

Frédéric Daigne

Institut d'Astrophysique, 98 bis Boulevard Arago, Paris 75014, France and Université Pierre et Marie Curie – Paris VI, 4 place Jussieu, 75005 Paris, France

daigne@iap.fr

Keith A. Olive

William I. Fine Theoretical Physics Institute, School of Physics and Astronomy, University of Minnesota, Minneapolis, MN 55455 USA

Elisabeth Vangioni-Flam

Institut d'Astrophysique, 98 bis Boulevard Arago, Paris 75014, France

Joseph Silk

Department of Physics, University of Oxford, Keble Road, Oxford OX1 3RH, and Institut d'Astrophysique, 98 bis Boulevard Arago, Paris 75014, France

and

Jean Audouze

Institut d'Astrophysique, 98 bis Boulevard Arago, Paris 75014, France

ABSTRACT

Motivated by the WMAP results indicating an early epoch of reionization, we consider alternative cosmic star formation models which are capable of reionizing the early intergalactic medium. We develop models which include an early burst of massive stars (with several possible mass ranges) combined with standard star formation. We compute the stellar ionizing flux of photons and we track the nucleosynthetic yields for several elements: D, ^{4}He, C, N, O, Si, S, Fe, Zn. We compute the subsequent chemical evolution as a function of redshift, both in the intergalactic medium and in the interstellar medium of forming galaxies, starting with the primordial objects which are responsible for the reionization. We apply constraints from the observed abundances in the Lyman α forest and in Damped

Lyman α clouds in conjunction with the ability of the models to produce the required degree of reionization. We also consider possible constraints associated with the observations of the two extremely metal-poor stars HE 0107-5240 and CS22949-037. We confirm that an early top-heavy stellar component is required, as a standard star formation model is unable to reionize the early Universe and reproduce the abundances of the very metal-poor halo stars. A bimodal (or top-heavy) IMF (40 - 100 $M_{\odot}$) is our preferred scenario compared to the extreme mass range ($\gtrsim$ 100 $M_{\odot}$) often assumed to be responsible for the early stages of reionization. A mode of even more extreme stellar masses in the range ($\geq$ 270 $M_{\odot}$) has also been considered. All massive stars in this mode collapse entirely into black holes, and as a consequence, chemical evolution and reionization are de-correlated. The ionizing flux from these very massive stars can easily reionize the Universe at $z \sim 17$. However the chemical evolution in this case is exactly the same as in the standard star formation model, and the observed high redshift abundances are not reproduced. We show that the initial top-heavy mode, which originally was introduced to reionize the early Universe, produces rapid initial metal pollution. The existence of old, C-rich halo stars with high [O/Fe] and [C/Fe] ratios is predicted as a consequence of these massive stars. The recently observed abundances in the oldest halo stars could trace this very specific stellar population. The extreme mass range is disfavored and there is no evidence, nor any need, for a hypothesised primordial population of very massive stars in order to account for the chemical abundances of extremely metal-poor halo stars or of the intergalactic medium.

The combined population of early-forming, normal (0.1 - 100 $M_{\odot}$) and massive (40 - 100 $M_{\odot}$) stars can simultaneously explain the cosmic chemical evolution and the observations of extremely metal-poor halo stars and also account for early cosmological reionization.

Subject headings: Cosmology: theory — nuclear reactions, nucleosynthesis, abundances — stars: evolution — Galaxy: evolution

1. Introduction

With the recent release of WMAP data, we have without question, entered the age of precision cosmology. While many of the accurately determined cosmological parameters were found to have values consistent with a ΛCDM cosmology, the TE cross-correlation power spectrum is consistent with a large optical depth due to electron scattering, $\tau_e = 0.17 \pm 0.04$

(Kogut et al. 2003) which suggests a very early epoch ($z \simeq 20$) of reionization in the intergalactic medium (IGM). It is often suggested that reionization is due to a population of very massive stars forming in minihalos, cooled predominantly by H_2 (see Cen 2003a; Haiman & Holder 2003; Wyithe & Loeb 2003; Bromm 2004). It has also been suggested that this early period of reionization is not total, but rather is regulated by radiative feedback effects delaying the complete reionization to a later redshift ($z \simeq 6$) accounting for the observed Gunn-Peterson trough (Becker et al. 2001).

Even a relatively brief period of massive star formation at high redshift can have dramatic consequences on the chemical enrichment of the primitive structures and of the IGM. There has been significant progress in our understanding of the yields of massive stars, particularly for so-called pair-instability supernovae, allowing one to trace the chemical history as influenced by an early massive population of stars. If indeed the first generation of stars were very massive (140-260 $M_\odot$), they would act as prompt initial enrichment sources for the IGM as well as the progenitors of galaxies such as our own. In addition, they would lay down a very distinct chemical signature which can be compared with other potential initial mass functions for the first generation of stars capable of producing the required degree of reionization.

The argument for a prompt initial enrichment laying down the seeds for the chemical evolution of the Galaxy is an old one going back to Truran & Cameron (1971). This notion receives confirmation in observations of r-process elements as a function of [Fe/H] in halo stars (Wasserburg & Qian 2000; Qian & Wasserburg 2001). The question of the ionization capacity of the massive stars supposed to produce this initial enrichment was recently considered by Oh et al. (2001), Oh (2002), and Venkatesan & Truran (2003) in the context of a late period of reionization at a redshift $z \sim 6$. More recently, metallicity studies of Damped Lyman α clouds (DLAs) at high redshift also indicate the presence of an initial metallicity of roughly [Fe/H] $\sim 10^{-3}$ (Prochaska et al. 2003). Tumlinson, Venkatesan, & Shull (2004) examined this question in the context of an early period of reionization as indicated by the WMAP data and present a general discussion of the initial mass function (IMF) of the first stars and their associated nucleosynthesis. Specifically they use the measured element abundances in the metal-poor halo stars to derive the IMF of population III stars responsible for the reionization of the early IGM. While our goal here is similar, we include a comprehensive model of chemical evolution to address this question.

Related to the question of an early population (Pop III) generation of stars is the observation of extremely metal-poor ([Fe/H] $<$ -4) stars such as HE 0107-5240 (Christlieb et al. 2004 and Bessell, Christlieb, & Gustafsson 2004), a halo giant which is extremely metal-poor, [Fe/H] = -5.3. While the abundances of other observed elements, e.g., Na, Mg, Ca, etc.

are (roughly) as low, the abundance of C (and N and O) is surprisingly high, [C/H] ≈ -1.3 ([N/H] ≈ -3.0, [O/H] ≈ -2.9). Indeed the very existence of this star poses a challenge for both models of chemical evolution (and also stellar evolution) and star formation as its mass is believed to be quite low ($M \sim 0.8$ $M_\odot$). We note, however, that it is possible that this star (and other similar stars such as CS 22949-037, Depagne et al. 2002 and Israelian et al. 2004) was born under very particular circumstances as these abundance patterns may be explained by the pre-enrichment of a massive zero-metallicity star (with fall-back) (Umeda & Nomoto 2003; see also Suda et al. 2004), or perhaps the star was polluted by a binary companion in its AGB phase. Thus with some degree of caution, we will discuss the implications of the existence of this star with respect to the models considered.

While there have been several detailed studies concerning the ionization efficiency of massive stars, attention to chemical enrichment has focused on the overall metallicity produced in structures with massive or very massive stars. Here, we calculate the combined effect of an early population of massive stars on the reionization history and chemical enrichment history of the early cosmic structures and of the IGM. In the framework of the hierarchical galaxy formation model, most of the halo, and in particular a DLA, is built up by smaller merging systems that are tidally disrupted (see e.g. (Zentner & Bullock 2003)). Therefore, they inherit the metals produced at large z by population III stars as a Prompt Initial Enrichment (PIE). The intensity of this PIE must be limited to avoid a metallicity surpluss in these late structures which produce new metals via the normal mode of star formation. Thus our approach is the following : (i) since the metallicity increases very rapidly as soon as the first population III stars explode, the timescale of the massive mode of star formation is necessarily short (see section 4.3); (ii) therefore, the cosmic SFR at $z \lesssim 5-6$ reflects only the normal mode of star formation. This allows one to normalize its intensity to fit the observed cosmic SFR at these redshifts ; (iii) once this normalization has been done, the metal production by the normal mode is immediately derived without any other parameter adjustement; (iv) from the amount of metals produced by the normal mode, it is then possible to estimate the maximum permitted initial metallicity in the structures at the beginning of the normal mode to avoid the over-production of metals in the late structures; (v) finally, this allows us to normalize the intensity of the early massive mode (pop. III stars) as it governs the PIE. We consider several initial mass functions which differ primarily in the population of massive stars forming at zero (or near zero) metallicity. Given an initial mass function and an associated star formation rate, we calculate in a consistent way both the chemical history of the cosmic structures and of the IGM as well as the efficiency for its reionization. Compared to previous studies, we do not restrict our discussion to the global metallicity but we specifically follow several chemical elements (D, ^{4}He, C, N, O, Si, S, Fe, Zn). We further discuss the implications of the observation of the extremely metal poor star ([Fe/H] = -5.3), HE 0107-5240. This star can severely constrain such models and/or models of stellar nucleosynthesis, particularly those for extremely massive stars which evolve through pair instability.

We find that a bimodal (or top-heavy) IMF (40 - 100 $M_\odot$), for example as discussed by Ciardi et al. (2003), is preferred over a scenario which includes a component with very massive stars ($\gtrsim$ 100 $M_\odot$) which are often assumed to be responsible for the early stage of reionization. The best model is well suited to account for C and Zn abundances, as well as Fe, O, Si and S in the DLAs, in the metal-poor IGM, and in the oldest halo stars. Furthermore, in order to reionize the universe at $z \sim 17$, we require an escape fraction for ionizing photons of only about 5 %. In contrast, we find that the massive starburst model, relying mostly on pair instability supernovae (PISNae) from stars in the range 140–260 $M_\odot$, requires a lower SFR intensity due to the overproduction of metals and as a consequence, the UV flux is weaker and requires a higher escape fraction of ionizing photons ($\sim$ 30 %) to achieve early reionization. Note that Venkatesan & Truran (2003) have also found a low ionizing efficiency for very massive stars. Nevertheless, the overproduction of some α–elements (specifically S and Si) seems unavoidable in these models. Moreover due to the specific yields of these PISNae, the observations of the metal-poor halo stars are not reproduced. We also consider a model with an extremely massive component, i.e., with a stellar mass range $\geq$ 270 $M_\odot$. Assuming that these massive stars collapse entirely into black holes in this mode, chemical evolution and reionization are de-correlated. We find that the ionizing flux from these very massive stars can very easily reionize the Universe at $z \sim 17$. However we also find that the resulting chemical evolution in this model is exactly the same as in a standard star formation model, and the high redshift abundances are not reproduced.

The outline of the paper is as follows: in section 2, we describe the chemical evolution models in detail, and our method for calculating the chemical enrichment inside the structures and the IGM. In section 3, we describe our computation of the flux of ionizing photons. Our results are collected in section 4 and our conclusions are summarized in section 5.

2. Chemical Evolution Models

While observations of stellar mass distributions are able to fix the present-day IMF quite well, one is required to apply observations of a wide range of element abundances in order to constrain the combined star formation rate and IMF throughout the history of Galaxy. When one goes beyond galactic chemical evolution, recent observations of the cosmic star formation rate (through the cosmic luminosity function) (Lanzetta et al. 2002; Nagamine et al. 2003, and references therein), and the abundances of heavy elements in quasar absorption systems enable one to place constraints on models up to a redshift of a few (Pettini et al. 2002; Pettini 2003; Ledoux et al. 2003; Prochaska et al. 2003; Centurión et al. 2003). In contrast, there have been very few constraints on the very first epoch of star formation concerning the IMF and SFR. The recent discovery of a candidate $z = 10$ galaxy (Pelló et al. 2004; Ricotti et al. 2004) indicates that this observational situation may improve rapidly.

As noted above, one of the most startling results of the 1st-year WMAP analysis is related to the ionization history of the Universe. It is often claimed that achieving a high degree of ionization at a redshift $z \simeq 20$, requires a very early generation of massive stars. A burst of massive star formation would have rather dramatic effects on the chemical history of the Universe. Not only would such a population of stars lay down an initial metal enrichment for the IGM, they would, depending on the IMF, lay down a very distinct fingerprint based on the abundances of elements produced by these stars. In particular, one could expect that the element abundance patterns determined by very massive stars ($\gtrsim 100$ $M_\odot$) would look very different from that of a normal IMF or even one biased by massive stars with masses in the typical range 10 - 100 $M_\odot$.

To test this hypothesis, we will consider several types of chemical evolution models. A basic review of chemical evolution models can be found in Tinsley (1980). In this paper, we present an extension of this standard formalism, where we now take into account two gas reservoirs, one accounting for the IGM and one for the interstellar medium (ISM) of the forming galaxies. This allows one to obtain high-redshift abundances, measured both in DLAs and in the Lyman-α forest. Galaxies form hierarchically, and the building blocks are defined by the fact that baryons must be able to cool in the dark matter halos. The minimum scale is about 10^6 $M_\odot$, and these objects first condense at about $z \sim 20$. However for the purposes of chemical evolution and reionization, we can avoid any detailed discussion of the mass function by restricting ourselves to integrated quantities such as condensed baryonic mass and the gas accretion rate, and to key parameters such as the escape fraction of ionizing photons, the star formation efficiency and the chemical yields.

Each model will be defined by several parameters : (i) the initial redshift at which star formation begins, $z_{\rm init}$. We adopt $t = 0$ at this redshift and relate the age at redshift z of a star formed at $z = z_{\rm init}$ by

$$\frac{dt}{dz} = \frac{9.78\ h^{-1}\ \mathrm{Gyr}}{(1+z)\sqrt{\Omega_\Lambda + \Omega_{\rm m}(1+z)^3}}\ ,$$

where we adopt $\Omega_\Lambda = 0.73$, $\Omega_{\rm m} = 0.27$ and $h = 0.71$ (Spergel et al. 2003). Notice that the quantity plotted in the figures in this paper is not the time t but the age of the Universe, which is $t + t_{\rm init}$, where the constant $t_{\rm init}$ is the age of the Universe at $z = z_{\rm init}$. (ii) the star formation rate (SFR), $\psi(t)$; (iii) the initial mass function (IMF), $\phi(m)$, for $m_{\rm inf} \leq m \leq m_{\rm sup}$. The IMF is normalized such that

$$\int_{m_{inf}}^{m_{sup}} dm \; m\phi(m) = 1 \; ; \tag{1}$$

(iv) the cosmic baryon accretion rate $a_{\rm b}(t)$, which accounts for the increase in the fraction of baryons in structures that have deep enough potential wells for hydrogen to be ionized, from an initial fraction of $a_{\rm init} \sim 1$ % at $z = 20$ in mini-halos (cf. Mo & White 2002) to the present value at $z = 0$ in galaxies of $\sim 10 - 15\%$ derived by Fukugita, Hogan, & Peebles (1998) and Dickinson et al. (2003); (v) the gas outflow from the cosmic structures $o(t)$.

The evolution of the gas mass in the IGM is given by:

$$\frac{dM_{\rm igm}}{dt} = -a_{\rm b}(t) + o(t) \; . \tag{2}$$

We consider two possible parametrizations of the cosmic baryon accretion rate $a_{\rm b}(t)$: (i) very localized structure formation at time t_0:

$$a_{\rm b}(t) = aM_{\rm tot} \; \delta(t - t_0) \; ;$$

and (ii) an exponentially decreasing formation rate starting at $t = 0$:

$$a_{\rm b}(t) = \frac{a}{\tau_{\rm s}} \; M_{\rm tot} \; \exp\left(-t/\tau_{\rm s}\right) \; ,$$

where the total mass $M_{\rm tot} = M_{\rm igm} + M_{\rm struct}$ is constant in the simulation and the mass of the structures evolves as

$$\frac{dM_{\rm struct}}{dt} = a_{\rm b}(t) - o(t) \; .$$

Initially $M_{\rm struct}/M_{\rm tot} = a_{\rm init}$ as defined above. In both cases, the constant a is the fraction of the total mass which is eventually accreted by the structures. It is adjusted to have the correct final value of the baryon fraction in the cosmic structures. In all of the models discussed below, we have chosen $a = 10$ %. In the second case, $\tau_{\rm s}$ is the timescale of the accretion process by the structures : 95 % of the accretion process is finished at $t \sim 3 \; \tau_{\rm s}$. As structure formation is not well constrained observationally at high z, we consider a large sample of timescales and show how they are constrained. Below we have considered four possible timescales : $\tau_{\rm s} = 0.01$, 0.2, 0.5 and 1 Gyr.

The outflow contains two terms $o(t) = o_{\rm w}(t) + o_{\rm sn}(t)$. The first one, $o_{\rm w}(t)$, is a global outflow powered by the stellar explosions (galactic wind). This term is similar to that described in Scully et al. (1997). The mass ejection rate by the wind is given by

$$o_{\rm w}(t) = \epsilon \int_{\max{(8 \; {\rm M}_\odot ; m_{\rm d}(t))}}^{m_{\rm up}} dm \; \phi(m)\psi\left(t - \tau(m)\right) \frac{2E_{\rm kin}(m)}{v_{\rm esc}^2(m)} \; , \tag{3}$$

where m_{up} is the upper mass limit of stars which expire as a supernova event and $m_{\rm d}(t)$ is the mass of a star which dies at age t. $E_{\rm kin}(m)$ and $v_{\rm esc}(m)$ are respectively the kinetic energy and the terminal velocity of the ejecta for a progenitor of mass m obtained from Woosley & Weaver (1995); Heger & Woosley (2002), and $\tau(m)$ is the main sequence lifetime of a star of mass m, taken here to be independent of metallicity. The fraction of the energy available to drive the wind, $\epsilon = 0.02$, is taken to be constant. The second term, $o_{\rm sn}(t)$ corresponds to the fraction α of stellar supernova ejecta which is flushed directly out of the structures, resulting in metal-enhanced winds as first proposed by Vader (1986):

$$o_{\rm sn}(t) = \alpha \int_{\max{(8~{\rm M}_\odot ; m_{\rm d}(t))}}^{m_{\rm up}} dm~\phi(m) \psi\left(t - \tau(m)\right)\left(m - m_{\rm r}\right)~,$$

where $m_{\rm r}$ is the mass of the leftover remnant and the fraction $\alpha = 0.005$ is also taken to be constant. Thus, as one can see, $o_{\rm w}(t)$ carries the chemical composition of the ISM, whereas $o_{\rm sn}(t)$ has the chemical composition of the supernovae.

The evolution of the gas mass in the structures is given by:

$$\frac{dM_{\rm ism}}{dt} = \left(-\psi(t) + e(t)\right) + \left(a_{\rm b}(t) - o(t)\right)~. \tag{4}$$

The stellar mass in the structures is of course given by the difference $M_{\rm struct} - M_{\rm ism}$. In equation (4), the second parenthesis accounts for the baryon exchange between the IGM and the structures, whereas the first parenthesis is the classical term related to the star formation. Specifically, the rate at which gas is returned to the ISM by mass loss or stellar deaths either in supernova events or in planetary nebulae, $e(t)$, is calculated including the effect of stellar lifetimes (delaying enrichment, though these effects are negligible for extremely massive stars), that is, we do not employ the instantaneous recycling approximation. Therefore $e(t)$ is given by :

$$e(t) = \int_{m_{\rm d}(t)}^{m_{up}} dm~\phi(m)\psi(t-\tau(m))(m - m_{\rm r})~. \tag{5}$$

Notice the distinction between $m_{\rm sup}$, the upper mass limit of stars which can form, and $m_{\rm up}$ which has been defined above. It has been suggested (Larson 1986; Olive, Thielemann, & Truran 1987) that one way to avoid the overproduction of ^{16}O in chemical evolution models is to limit the maximum mass of stars which will give a supernova. Stars more massive than this are assumed to collapse entirely into black holes returning no material to the ISM. This idea is now supported by the recent calculation of Heger & Woosley (2002) (see below). As we will see this distinction may be quite important for very massive stars required for ionization, but may be problematic from the point of view of chemical enrichment.

The chemical evolution of a specific element i is also given by two equations, one for the mass fraction in the IGM, $X_i^{\rm igm}$, and one for the mass fraction in the ISM of the cosmic structures, $X_i^{\rm ism}$:

$$\frac{dX_i^{\rm igm}}{dt} = \frac{1}{M_{\rm igm}(t)}\left[o_{\rm w}(t)\left(X_i^{\rm ism}(t) - X_i^{\rm igm}(t)\right) + \left(o_{{\rm sn},i}(t) - o_{\rm sn}(t)X_i^{\rm igm}(t)\right)\right] \ , \tag{6}$$

$$\begin{aligned}\frac{dX_i^{\rm ism}}{dt} \ &= \ \frac{1}{M_{\rm ism}(t)}\left[\left(e_i(t) - e(t)X_i^{\rm ism}(t)\right)\right.\\ &\left. +a_{\rm b}(t)\left(X_i^{\rm igm}(t) - X_i^{\rm ism}(t)\right) - \left(o_{{\rm sn},i}(t) - o_{\rm sn}(t)X_i^{\rm ism}(t)\right)\right] \ ,\end{aligned} \tag{7}$$

where $o_{{\rm sn},i}/o_{\rm sn}$ is the mass fraction of element i in the supernova ejecta which are directly ejected in the IGM and therefore do not contribute to the chemical enrichment of the structures, and $e_i(t)$ is the rate at which element i is ejected by stars into the ISM. It is given by

$$e_i(t) = \int_{m_{\rm d}(t)}^{m_{up}} dm \ \phi(m)\psi(t - \tau(m))m_i^{\rm ej}(m). \tag{8}$$

The ejected mass of element i by a star of initial mass m, $m_i^{\rm ej}(m)$, is computed from the stellar yields. Despite the fact that this dependence has not been explicitly written in equations (5) and (8), the mass of the remnant $m_{\rm r}$, the ejected mass of element i, $m_i^{\rm ej}$, and for the massive stars the kinetic energy $E_{\rm kin}$ and the terminal velocity $v_{\rm esc}$ of the supernova ejecta are functions not only of the initial stellar mass m, but also of its initial metallicity, which is taken to be the metallicity of the ISM at time $t - \tau(m)$. Notice that for the specific case of iron, we add a term accounting for the production of radioactive nickel by type Ia supernovae, assuming that they typically occur with a delay of 1 Gyr and they produce 0.5 $M_\odot$ of nickel per event.

We have divided the stellar mass range in three domains : (i) for intermediate mass stars (< 8 $M_\odot$), the remnant is always a white dwarf. We adopt stellar lifetimes from Maeder & Meynet (1989). The stellar yields and the mass of the white dwarfs are taken from van den Hoek & Groenewegen (1997) for stars with masses in the range 0.9 - 8 $M_\odot$ and metallicity in the range Z = 0.0001, 0.004, 0.008, 0.02; (ii) for massive stars ($8 < m < 100$ $M_\odot$), we adopt stellar lifetimes from Schaerer (2002). We take the nature of the remnant (neutron star or black hole) from Heger et al. (2003) and the stellar yields as well as the mass of the remnant from Woosley & Weaver (1995) for stars with mass in the range $12 - 40$ $M_\odot$ and metallicity in the range $Z/Z_\odot = 0$, 0.0001, 0.01, 0.1, 1. Specifically we use the results of their model B using a kinetic energy $E_{\rm kin} \sim 2 \times 10^{51}$ erg for $m = 30$, 35 and 40 $M_\odot$, as this model leads to a better agreement with the observed abundance ratios in extremely-metal poor halo stars (see section 4.3). The maximum initial stellar mass studied in their paper is 40 $M_\odot$, which necessitates an extrapolation for $40 < m < 100$ $M_\odot$. We note that the slope of the IMF favors stars with lower masses, which means that the contribution of stars close to 100 $M_\odot$ is always very small in all our models. For the same reason, the arbitrary choice of 100 $M_\odot$ as maximum mass is of little influence. Our results would be unchanged with a maximum mass of 140 $M_\odot$; (iii) finally for very massive stars (> 140 $M_\odot$), we use the recent calculations of Heger & Woosley (2002), which predict that stars end as a so-called PISN for $140 < m < 260$ $M_\odot$ and entirely collapse into a black hole for $m > 260$ $M_\odot$. The corresponding stellar yields are taken from the same paper. We adopt the stellar lifetimes from Schaerer (2002). Note also that for $m < 100$ $M_\odot$, the evolution of the metallicity dependence is taken into account by an interpolation between the sets provided in the studies cited above.

We investigate several scenarios of cosmic star formation:

1. A Standard model ("Model 0")

   The standard model which we use to compare the more speculative models involving very massive stars is defined by an IMF with a slope slightly steeper than that of a Salpeter mass function (x = 1.35)

$$\phi(m) \propto m^{-(x+1)} \qquad x = 1.7 \tag{9}$$

   for stellar masses between 0.1 and 100 $M_\odot$ (Scalo 1986), and a star formation rate (SFR) proportional to the gas mass fraction in the cosmic structures, $\sigma(t)$,

$$\psi(t) = \nu_1 \sigma(t) \ , \tag{10}$$

   where $\nu_1 = M_{\rm struct}(t)/\tau_1$ with $\tau_1 = 5$ Gyr, which is the typical timescale for star formation in the galactic disk. The overall (late) evolution of the chemical abundances are quite acceptable in this model. However, as we shall see, this model can not explain the rather peculiar nature of the extreme metal poor star HE 0107-5240 nor can this model achieve the necessary degree of ionization at high redshift.

2. A massive mode added to a standard-like model ("Model 1")

   In this case, we consider an epoch of massive star formation with a power-law IMF as in eq. (9) but with a range 40 - 100 $M_\odot$. The brevity of this period of star formation is governed by the SFR which is taken here to be an exponential,

$$\psi(t) = \nu_2 \ e^{-t/\tau_2}, \tag{11}$$

   where $\tau_2 = 50$ Myr is the characteristic timescale of this massive starburst and $\nu_2 = f_2 \ M_{\rm struct}(t)/\tau_2$. The fraction f_2 equals 4.5 % so that $\nu_2 = \left(0.9 \ {\rm Gyr}^{-1}\right) M_{\rm struct}(t)$.

This short period of star formation activity acts as a prompt initial enrichment of the cosmic structures which leads rapidly to a metallicity as high as 10^{-3} $Z_{\odot}$ and at the same time provides ample energy for the ionization of the IGM. In this context, the possible delay between the massive and normal SFR is required to be very short (of the order of the lifetime of a typical massive star, a few $\times 10^6$ yrs). So there is no significant difference between the simultaneous combination of the two modes or the introduction of this short delay which affects any correlation between nucleosynthesis and the rate of ionization. This delay can account for a period of negative feedback due to the lack of neutral H_2 necessary for cooling (Bromm 2004). The chemical history of the elements is in good agreement with observables between $z = 5$ to $z = 0$, including the essential of observations of HE017-5240.

3. Pair Instability SN mode ("Model 2a")

   We also consider a more extreme case, where the initial massive mode (once again given by the same power-law IMF) covers stellar masses in range 140 - 260 $M_{\odot}$, corresponding to the so-called Pair Instability supernovae. We take the same SFR as in eq. (11) and the yields are taken from Heger & Woosley (2002).

   In this model, for the same SFR intensity, we find a larger production of metals than we did in case 2 due to the fact no remnant is left behind and all of the enriched stellar mass is returned to the ISM and IGM. In this context, we must lower the SFR of the massive mode by a factor of about 8 in order to avoid the overproduction of metals in the ISM. Consequently, the ionizing efficiency is lower than in case 2. Finally, due to the specific nucleosynthesis ascribed to PISNae, we can not reproduce the abundance patterns (e.g., of C, N, Zn) found in the data of the HE 0107-5240.

4. Black hole mode ("Model 2b")

   Finally we consider a mode where the massive IMF covers stellar masses in the 270 - 500 $M_{\odot}$ range. All of these stars are assumed to collapse entirely to black holes without contaminating the environment. Indeed, the ill effects on the production of heavy elements by the extreme massive component of the case 3 can be ameliorated if it is assumed that these stars provide only a source of ionization. In this case, there is a de-correlation between global chemical evolution and reionization. Chemical enrichment could proceed solely through the normal component. Although this mode fit observed abundances well at late times, it does not fit the abundances which are characterized by HE 0107 5240 at low [Fe/H]. We further note that the SFR of this very massive mode is in principle constrained from above, and hence we can not adjust it arbitrarily to obtain reionization. Indeed, if a large fraction of the baryons in the structures was trapped in black holes, the remaining reservoir to form stars would not be sufficient to fit the observed cosmic SFR. Moreover, the intensity of this early burst of very massive stars, governed by the fraction f_2, must also be limited so that the contribution to the cosmic SFR at $z \simeq 5-6$ of the tail of this massive mode remains negligible.

3. Reionization

The ionizing flux from the stars is entirely dominated by the contribution of massive stars with short lifetimes. Therefore, it is a good approximation to consider that the total number of UV photons emitted by a star of initial mass m, $N_\gamma(m)$, is entirely emitted impulsively when the stars dies. Then the ionizing flux is given by

$$\frac{dn_\gamma}{dt} = \int_{m_{\rm d}(t)}^{m_{\rm sup}} dm\ \phi(m)\psi\left(t-\tau(m)\right) N_\gamma(m)\ . \tag{12}$$

We do not distinguish the reionization of hydrogen and helium in this paper, and hence, we consider all UV photons with $h\nu \geq 13.6$ eV. We adopt the values of $N_\gamma(m)$ for stars with masses in the range 5–500 $M_\odot$ computed by Schaerer (2002) at zero metallicity. Only a fraction $f_{\rm esc}$ of these ionizing photons will escape the structures and contribute to the reionization of the IGM. To a first approximation, we consider in this paper that $f_{\rm esc}$ is constant, for lack of any better model. Estimates of $f_{\rm esc}$ range from ~ 0.03 to ~ 0.5, the former applying to nearby star-forming galaxies and the latter applying to Lyman break galaxies at $z \sim 3$ (Steidel, Pettini, & Adelberger 2001). Note that we do not include any photon-ionization feedback on the star formation as this effect is expected to be weak at very high redshifts (Oh & Haiman 2003; Dijkstra et al. 2004b).

In a forthcoming paper, we will perform the detailed calculation of the reionization process in the IGM, taking into account the balance between the ionizing flux and the recombination rate for each species (H^+, He^+ and He^{++}). In this paper we adopt a simplified criterion to decide whether our stellar population is able to reionize the early Universe or not. We estimate the mean recombination time $\langle t_{\rm rec}\rangle$ of an atom ionized at redshift z using (Ricotti & Ostriker 2004)

$$\frac{\langle t_{\rm rec}\rangle}{t_{\rm H}} = 0.046\ \left(\frac{1+z}{18}\right)^{-1.5}\ \left(\frac{C_{\rm H\,II}}{10}\right)^{-1}\ , \tag{13}$$

where $t_{\rm H}$ is the Hubble time at redshift z and $C_{\rm H\,II}$ is the clumpiness factor of the ionized regions, whose evolution with redshift remains quite uncertain. We can estimate the number of ionizing photons per intergalactic baryon necessary to fully reionize the IGM at redshift

z with

$$\begin{aligned} n_{\gamma,\ \rm min} &= \left(\frac{\langle t_{\rm rec}\rangle}{t_{\rm H}}\right)^{-1} = 22\ \left(\frac{1+z}{18}\right)^{1.5}\ \left(\frac{C_{\rm H\ II}}{10}\right)\ \text{ph/b if}\ \ \langle t_{\rm rec}\rangle < t_{\rm H} \\ &= 1\ \text{ph/b otherwise} \end{aligned} \tag{14}$$

As such, we will consider that early reionization at $z \sim 17$ is fully achieved only if the structures have cumulatively ejected $\sim 10 - 20$ ionizing photons per intergalactic baryon by the end of the initial massive starburst (i.e. typically for $z_{\rm init} = 20$). While the reionization redshift increases with the number of ionizations per photon, it is reduced by the mean clumpiness of the IGM. If the first generation of stars formed in isolated star cluster-mass structures, which seems plausible at high redshift in a hierarchical model of structure formation, $f_{\rm esc}$ is likely to be high (Ricotti 2002). We therefore conservatively take as the required production rate of ionizing photons per baryon a number of about 10. See for example a recent discussion (Dijkstra, Haiman, & Loeb 2004a) that estimates ~ 10 ionizations per intergalactic baryon are needed to maintain a constant ionization fraction for a specified optical depth taken equal to the WMAP estimate and a clumpiness factor of the IGM $\langle n^2\rangle/\langle n\rangle^2 \sim 3$.

4. Results

In this section we display and compare the results of the models considered. We will discuss in turn, the star formation rate, the ionization flux and the chemical evolution of the element abundances. In all of the models considered, star formation begins at $z_{\rm init} = 20$.

4.1. The Star Formation Rate

We begin by first comparing the results for each of the models with respect to their predicted star formation history. As discussed above we will consider several scenarios for the time evolution of the baryon accretion rate. In Model 0, we both adopt a uniform baryon accretion rate between $z = 20$ and $z = 0$ and an exponentially decreasing baryon accretion rate with several timescales $\tau_{\rm s}$: 0.01, 0.2, 0.5 and 1 Gyr. For models 1 and 2, we consider only the latter, however in the case of Model 1, we also show the effect of a delta function at $z = 6$ (late and rapid structure formation).

In Figure 1 we show the evolution of the cosmic star formation rate for Model 0, and compare it to recent observations (deduced from luminosity functions) (Nagamine et al. 2003, and references therein). We plot the comoving star formation rate in units of $\mathrm{M_\odot yr^{-1} Mpc^{-3}}$ which is related to $\psi(t)$ by

$$\mathrm{SFR}\ (\mathrm{M_\odot yr^{-1} Mpc^{-3}}) = \rho_\mathrm{b}\ (\mathrm{M_\odot Mpc^{-3}})\ \times\ \frac{\Psi(t)}{M_\mathrm{tot}}\ (\mathrm{yr^{-1}}),$$

where $\rho_\mathrm{b} = 2.77 \times 10^{11}\ (\Omega_\mathrm{b} h^2)\ \mathrm{M_\odot Mpc^{-3}}$ is the comoving baryon density in the Universe. We take $\Omega_b = 0.044$. With the exception of the constant accretion rate ($\tau_\mathrm{s} = \infty$, shown as the dotted curve) all of the models with $\tau_\mathrm{s} = 0.01 - 1.0$ Gyr reproduce the observed rise of the SFR between $z = 0$ and $z = 5$. Note that in the case of a constant accretion rate ($\tau_\mathrm{s} = \infty$), slower structure formation necessitates an intrinsically more efficient rate of star formation in order to correctly reproduce the global chemical evolution history. Therefore we have multiplied the initial SFR intensity by a factor of ~ 5 so that $\tau_1 = 1$ Gyr for this case. This explains why in Figure 1 the initial value of the dotted curve is ~ 5 times larger than it is for the other models.

Despite the large observational uncertainty, the shape of the observed SFR up to $z = 5$ allows us to constrain the completion time scale for the formation of structures, i.e. $\tau_\mathrm{s} \lesssim 1$ Gyr. When this constraint is satisfied, Model 0 is in good agreement with the observed behaviour of the SFR at late times ($z < 5$). On the other hand, the lack of data at high redshift does not allow one to distinguish between rapid ($\tau_\mathrm{s} = 0.01$ Gyr) and prolonged ($\tau_\mathrm{s} \sim 0.2 - 0.5$ Gyr) structure formation. The recent discovery of a candidate $z = 10$ galaxy (Pelló et al. 2004; Ricotti et al. 2004) indicates that SFR determination at $z \leq 10$ should become available soon.

The bimodal SFR defining Model 1 is a linear combination of the normal mode used in Model 0 and a second mode, favouring massive stars at the onset of star formation. This massive mode is characterized by a SFR which is not coupled to the gas fraction in the structures but is simply exponentially decreasing with a timescale $\tau_2 = 0.05$ Gyr and a lower mass limit of the IMF, $m_\mathrm{inf} = 40\ \mathrm{M_\odot}$. Figure 2 shows the cosmic SFR obtained in Model 1 for three possible histories of structure formation. As in Model 0, we consider an exponentially decreasing baryon accretion rate with timescales $\tau_\mathrm{s} = 0.01$ or 0.2 Gyr. Compared to Figure 1, where the initial value of the SFR is $1.2 \times 10^{-2}\ \mathrm{M_\odot yr^{-1} Mpc^{-3}}$, the initial value of the SFR in Figure 2 equals $6.7 \times 10^{-2}\ \mathrm{M_\odot yr^{-1} Mpc^{-3}}$, which corresponds to an increase by a factor $(\nu_2 + \nu_1)/\nu_1 = 5.5$ due to the contribution of the massive mode. We also consider a model in which the accretion occurs instantaneously to model a burst of star formation relatively late at $z = 6$ (this model is quoted as "delta-function at $z = 6$" in Figure 2). As we see, the late time evolution of the models is dominated by the normal mode. For this reason, as in Model 0, the observed SFR is well reproduced in all of the scenarios for $z \lesssim 5$. As noted above for Model 0, it is impossible to distinguish between the three scenarios on the basis of SFR observations alone. However we will see in section 4.2 that the early ionizing flux in the case of instantaneous late structure formation is not able to ionize the IGM.

Models 2a and 2b have been considered in order to study the case of an initial starburst with a more extreme mass range. Model 2a corresponds to a starburst forming massive stars between 140 and 260 $M_\odot$, which is the domain where stars end their life as PISNae – the star is entirely destroyed leaving no remnant and a very large amount of metals is released into the ISM. In contrast, Model 2b corresponds to a even more massive domain, $270 \leq m \leq 500$ $M_\odot$ where stars collapse entirely into black holes, without any contribution to the metal enrichment of the surrounding gas. The SFR in both cases is taken to be the same as in Model 1, with a timescale $\tau_2 = 0.05$ Gyr. In this case, we only consider the fast structure formation mode ($\tau_\mathrm{s} = 0.01$ Gyr) as it optimizes the early emission of ionizing photons.

The two mass domains lead to very different results. In Model 2a, because of the intense production of metals by the PISN stars, it is necessary to decrease the intensity of the massive starburst by a factor of about 8 to avoid overabundances. Therefore we take $f_2 = 0.56$ % corresponding to $\nu_2 = \left(0.11 \text{ Gyr}^{-1}\right) M_\mathrm{struct}(t)$. As the late evolution is dominated by the normal mode, the computed cosmic SFR is still in good agreement with the observations, as can be seen in Figure 3. For Model 2b, Figure 3 corresponds to the maximum allowed starburst intensity which still allows the normal mode to dominate below $z = 5$.

4.2. The Ionization Flux

The structure formation timescale has a direct impact on the early ionizing flux of photons, as it governs the size of the gas reservoir for star formation. Therefore we restrict our attention to $\tau_\mathrm{s} = 0.01$ Gyr for Model 0, which optimizes this flux. However, even in this case, the number of ionizing photons produced at $z = 17$ (1.6 photons per baryon) is much too low to reionize the early Universe (see Figure 4). For this reason, we conclude that Model 0 can be rejected and that a massive mode is required.

Indeed, we see in Figure 4 the results for the ionizing photon flux for models 1 and 2 (a and b). The early ionizing flux is strongly dependent on the early structure formation history. In Model 1, our calculations show that it is only when structure formation is rapid (exponential decay with $\tau_\mathrm{s} = 0.01$ Gyr) that early reionization of the Universe is possible. Figure 4 shows indeed that in this case, 237 photons per baryon are produced at $z = 17$, which allows for reionization with a low value of $f_\mathrm{esc} \simeq 5$ %. In contrast, the case $\tau_\mathrm{s} = 0.2$ Gyr, which is not plotted, produces an integrated ionizing photon flux of only 55 photons per baryon. Even worse, the case of the late structure formation at $z = 6$ plotted in Figure 2 provides only 30 photons per baryon. Models with slow structure formation would then require a high value of $f_{\rm esc}$ (20-60 %).

In the case of Model 2a, the decrease of the massive starburst intensity discussed above has a large impact on the number of ionizing photons produced at $z = 17$. As seen in Figure 4, the flux is reduced to only 32 photons per baryon. This makes the early reionization of the Universe possible only if the fraction of photons that escape the structure is at least as high as 1/3. Model 2b, on the other hand, yields results which are very similar to those of Model 1. The resulting ionizing photon flux is, as expected, quite high : 282 photons per baryon at $z = 17$ which allows for the early reionization of the Universe even with an escape fraction of only $f_{\rm esc} \sim 3.5\%$. The similarity between the early production of ionizing photons in Models 1 and 2b is related to the constraint imposed on intensity of the initial starburst in Model 2b by the SFR (see Figure 3).

The capacity of Model 1 and Model 2b to reionize the IGM is confirmed in Figure 5, where we have plotted the cumulative number of ionizing photons as a function of redshift. We have also indicated the mean recombination time and the mean number of ionizing photons per baryon necessary to reionize the Universe at redshift z, as estimated using equations (13) and (14). The latter depends on the value of the clumpiness factor in H II regions (which has been assumed to be constant with z in this simple calculation). Model 2a marginally appears to be able to reionize the IGM early. However, this model suffers from an additional difficulty : the peak of the ionizing flux (see Figure 4) is reached at $z \sim 18-19$ where the metallicity is already as high as $Z/Z_\odot \sim 10^{-2} - 10^{-1}$. The possibility of forming stars with $m > 140$ M$_\odot$ at these high metallicities is questionable (see e.g. Schneider, Ferrara, Natarajan, & Omukai 2002; Bromm, Ferrara, Coppi, & Larson 2001a; Ricotti & Ostriker 2004). Although the metallicity in Model 1 is similar when the ionizing flux is maximum, it does not suffer this inconsistency as the IMF is truncated at $m = 100$ M$_\odot$, and star formation is not as inhibited when Z increases. On the other hand, the very massive IMF ($m > 270$ M$_\odot$) in Model 2 does not produce metals (see next section). Therefore the metallicity is only $Z/Z_\odot \sim 10^{-4} - 10^{-3}$ when the ionizing flux is maximum, i.e. consistent with a very massive IMF.

As discussed in the next section, constraints from chemical evolution require that the massive starburst finishes by $z \sim 8 - 10$. After which, the normal mode is dominant and is less efficient at ionizing the IGM (see Figure 4). However the ionization of the IGM at these redshifts can be maintained despite the reduced number of photons per baryon. Thus, it is not unlikely that a normal stellar population may account for the ionization level at $z \sim 6$, when the neutral gas fraction is $\gtrsim 0.001$ % (Oh 2002), as inferred from the observation of the Gunn-Peterson effect in the spectrum of high-redshift quasars. This possibility will be studied in a forthcoming paper presenting a detailed calculation of the reionization process.

4.3. Element Abundances

Next, we turn our attention to the resulting element abundances in the models considered. We note first that the evolution of the gas fraction in each of the models is quite similar as shown in Fig. 6. In contrast, the total metallicity is quite different in each case as seen in Fig. 7. In Fig. 7, we show the evolution of the total metallicity relative to solar metallicity in both the ISM of the growing structures and the IGM. We also show the data from 100 DLAs at $z \leq 4$ (Prochaska et al. 2003) which can be compared with the computed ISM metal abundance. As one might expect, Model 0 (and by definition Model 2b) produce very reasonable results. However, as we have just shown that the addition of an initial massive starburst is necessary for the early reionization of the Universe, it is now important to check that the cosmic chemical evolution is still consistent both with the local[1] and high redshift observed abundances. Figure 7 also shows that the metal enrichment is rapid in Model 1 : $Z = 10^{-3} - 10^{-2}\ Z_{\odot}$ immediately at $z = 20 - 19$ (see also Bromm 2004). As mentioned in the previous section, this justifies that the delay between the starting epochs of the two modes of star formation can be neglected in this context. The global metallicity in Model 2a is very similar to that in Model 1.

In Figs. 8 - 18, we show the resulting evolution of He, C, C/Fe, N, O, O/Fe, Si, S, Fe, Zn, and D. While there is no high redshift data to compare the He abundance to, Figure 8 shows an interesting signature of Model 1 compared to the others : a noticeable supplementary amount of Helium is produced at high redshift by the massive stars. The local value is however well fit. In Model 2a, only a small amount of Helium is produced because of the shift in stellar nucleosynthesis towards the heavy elements.

Despite the fact that the late chemical evolution of Model 0 is quite acceptable, the observed abundances of the star HE 0107-5240, if taken as representative of the very early epoch under consideration, are not reproduced, especially the Carbon and Oxygen to Iron ratios, as seen in Figures 10 and 13 where the observed level of these ratios is never attained. In addition the Carbon, Nitrogen, Oxygen and Sulfur abundances (Figures 9, 11, 12 and 15) are poorly fit. By that we mean that in this model, the abundance of Fe and Zn is reached at very high redshift ($z \sim 19$), as expected, whereas the abundance level of the other elements (C,N,O and S) is attained at a later epoch ($z \sim 12 - 16$). A good fit to the

[1] 'Local abundance' refers to the mean abundance at $z = 0$.

abundance pattern of this star would require the model to reach the observed abundance for each element at the same redshift. Therefore it seems that Model 0 can also be rejected on the basis of chemical criteria at high redshift.

Overall, the abundances predicted by Model 1 in the local structures are consistent with observations. The late evolution of the Silicon, Sulfur and Iron abundances in the cosmic structures (Figures 14, 15, and 16) is also in good agreement with the observations in DLAs (Pettini et al. 2002; Pettini 2003; Ledoux et al. 2003; Prochaska et al. 2003) and the late evolution of the Carbon and Silicon abundances in the IGM (Figures 9 and 14) is consistent with the observations in the Lyman-α forest (Songaila 2001). Notice however that Songaila (2001) measures the abundance of C IV and Si IV and does not apply any ionization correction. The work of Schaye et al. (2003) and Aguirre et al. (2004) indicates that the total abundance of C and Si could be a factor of $\sim$ 5-7 larger. The case of Oxygen is more problematic. The Oxygen abundance evolution predicted in Model 1 is in good agreement with the recent observations in massive star forming galaxies at $z \geq 2$ (Shapley et al. 2004). These observations clearly indicate little evolution of the Oxygen abundance from $z = 2$ to $z = 0$, and favor an early enrichment at $z > 2$. However, Figure 12 shows that Oxygen is overabundant when compared to the observations in DLAs (Pettini et al. 2002). One possible observational bias is related to the fact that the Oxygen abundance can be measured only if the observed lines are not saturated, which favors the weakest systems. On the other hand, a detailed study of the impact of the uncertainty in stellar yields should also be considered. Finally, Model 1 predictions in the IGM agree with the estimate of the Oxygen abundance in the Lyman-α forest (Simcoe et al. 2004). Note that only O VI is directly measured by these authors. Therefore their estimate of the total Oxygen abundance is limited by the uncertainties of the ionization state of Oxygen in these regions.

Moreover, if we adopt the extreme metal-poor halo stars HE 0107-5240 ([Fe/H]=-5.3) and CS 22949-037 ([Fe/H]=-4) as tracers of the very early Universe, it is remarkable that Model 1 is still globally consistent with the absolute abundances of Carbon, Oxygen, Silicon, Iron and Zinc (Figures 9, 12, 14, 16 and 17). The upper limit for the abundance of Sulfur which is available for HE 0107-5240 does not constrain the model. However the prediction of Model 1 is not in very good agreement with the abundance of Sulfur in CS 22949-037 (Figure 15). That is, the build-up of S occurs late in the model with respect to what is observed in this star. Similarly, the abundance of Nitrogen is reproduced in a satisfactory manner in HE 0107-5240 but not in CS 22949-037 (Figure 11) due to the extremely high abundance of N observed there.

We have also considered the predictions of Model 1 for the Carbon and Oxygen to Iron ratios, as these ratios are very specific for these extremely old halo-stars. The main quantity governing these ratios is the lower mass of the stars formed in the initial massive starburst. Figures 10 and 13 compare the results obtained for $m_{\rm inf} = 20$ M$_\odot$ in comparison with $m_{\rm inf} = 40$ M$_\odot$ which has been used elsewhere for Model 1. As our calculations use the stellar yields of Woosley & Weaver (1995) in this mass range, our results are directly related to the evolution of the amount of Carbon, Oxygen and Iron produced by stars from 20 M$_\odot$ to 40 M$_\odot$. In this context, Figures 10 and 13 show that $m_{\rm inf} = 40$ M$_\odot$ clearly favors high Carbon and Oxygen to Iron ratios, as observed in both HE 0107-5240 and CS 22949-037. Conversely, $m_{\rm inf} = 20$ M$_\odot$ favors the early production of Zinc as this element is not synthesized for $M > 30$ M$_\odot$ at low metallicity according to Woosley & Weaver (1995). In this case, Figure 17 shows a steeper increase of the Zinc abundance between $z = 20$ and $z = 17$. Finally, note that the local Zn abundance is not reproduced in any model, indicating the lack of Zn production in stellar models (Bihain et al. 2004). One can conclude that the observations of such stars provide strong constraints for both the IMF of Pop III stars and stellar models, specifically at zero metallicity.

We conclude that Model 1 satisfies quite well all of the available constraints : when we superimpose an initial massive starburst to the normal mode, we predict a UV photon flux which is clearly sufficient to reionize the early Universe together with cosmic chemical evolution in the structures and in the IGM which is globally consistent with the local abundances and the abundances measured in DLAs and in the Lyman-α forest, as well as in the extreme metal-poor halo stars. In addition, we predict that stars like HE 0107-5240 probably trace a generation of very old stars with a very specific chemical signature, and which were formed in the very first mini-halos and are thus well localized in time.

Next, we turn our attention back to Model 2a. The local abundances (C, O, N, Si, S and Fe) are still well reproduced. Compared to Model 1, the overabundance of Oxygen in the structures and in the IGM is reduced (see Figure 12) as was the case for He. However, Silicon, Sulfur and Iron are now a little over-abundant at late times (Figures 14, 15 and 16). The Zinc abundance is the same as in Model 1 at late times, showing a local underabundance. In the IGM, the Silicon abundance is better reproduced than in Model 1 but Carbon is underabundant (Figures 9 and 14). In conclusion, the late chemical evolution is globally less satisfactory than in Model 1. For the peculiar case of the extreme metal-poor halo stars, Figures 10 and 13 clearly prove that the predicted nucleosynthesis of PISN stars is unable to produce high Carbon and Oxygen to Iron ratios as observed in HE 0107-5240 and CS 22949-037.

Finally, Model 2b is a very peculiar case as stars above 270 M$_\odot$ emit a large amount of ionizing photons but produce no metals: the reionization process and the cosmic chemical evolution are now de-correlated. The only constraint on the intensity of the initial massive starburst comes from the observed cosmic SFR. Thus the chemical evolution is identical to that in Model 0 and therefore reproduces well the observed late evolution but cannot satisfy the constraints at high redshift coming from HE 0107-5240 and CS 22949-037. In light of this result, one can envision the possibility of a three-component model, based on Model 1 + a third massive component in the 270 – 500 $M_\odot$ range. The addition of this component, the intensity of which is limited by the cosmic SFR constraint, will only increase the early ionizing flux.

These results show clearly that observations do not support the hypothesis of the existence of an early very massive stellar population. All of the observational constraints are better reproduced by Model 1 with a massive mode in the range 40–100 $M_\odot$. Such a conclusion was recently obtained by Venkatesan et al. (2004) in a completely different astrophysical context : high redshift quasars with solar of higher metal abundances.

Before concluding this section, we would like to address the question of the evolution of D/H in the structures. Unlike the evolution of most other elements, the abundance of D/H decreases monotonically in time. The evolution of D/H in the models considered here is shown in Fig. 18. As one can see, in all models including Model 1, there is very little change in D/H at early times, At lower redshift, as D-free material is returned to the ISM, the D/H abundance begins to drop. In the figure, we compare the evolution of D/H to the deuterium abundance observed in quasar absorption systems. Previously, it was noted (Cassé et al. 1998) that there is a relation between the amount of deuterium destruction and the rise in the observed cosmic star formation rate. In the models considered there, the timescale over which the massive mode was operative was significantly longer than that considered here. Because of the necessity to reionize the Universe at very high redshift, the timescale associated with the massive mode in Models 1 and 2 is considerably shorter, thereby reducing the effect of the massive stars on the overall destruction of D/H.

The average observed D/H abundance is in very good agreement with the BBN predicted value of of D/H (Cyburt et al. 2003; Coc et al. 2004) based on the WMAP-inferred baryon density (Spergel et al. 2003), however, there appears to be considerable scatter in the data. While the scatter may be due to unresolved systematic uncertainties in the data, it may also be a signature of specific chemical evolution. In Fields et al. (2001), it was argued that significant changes in D/H could be achieved if there is an enhanced population of intermediate mass stars. The same model has also been used recently to explain (Ashenfelter, Mathews, & Olive 2004a,b) the apparent observations of variations in the fine-structure constant in the similar quasar absorption systems (Murphy et al. 2003; Chand et al. 2004). Although we have not presented the results here, we have tested the idea that intermediate mass stars ($\sim$ 3–8 $M_\odot$) dominated the IMF at $z \approx 20$ and have found that an enhanced population of intermediate mass stars could not provide enough ionizing photons to reionize the IGM. Thus, such a population, if it existed, would operate at later times after the prompt enrichment from massive stars as in Models 1 and 2.

5. Conclusions

It is likely that ionizing photons from stars, as opposed to say accreting black holes (in effect quasars or miniquasars) are responsible for the early epoch of reionization at $z \sim 15 - 20$ inferred from the WMAP results (cf. Dijkstra et al. 2004b). However there are severe limitations on massive stars if these formed with a "normal" IMF. The hypothesis of a generation of very massive metal-free stars helps supply the ionization requirements (Cen 2003a; Wyithe & Loeb 2003). However, we show here that chemical evolution constraints essentially rule out such an interpretation. Rather, we describe how a standard massive IMF (40-100 $M_\odot$), for example as discussed by Ciardi et al. (2003), can reionize the early intergalactic medium (see also a discussion of an even less massive IMF by Venkatesan & Truran 2003).

Our approach is to use the cosmic star formation rate history as our primary guide to early star formation rates, and work with integrated quantities in the context of hierarchical structure formation to yield the ionizing photon flux history for alternative cosmic star formation models which are capable of reionizing the early intergalactic medium. We have developed models which include an early burst of massive stars combined with standard star formation. We computed the stellar ionizing flux of photons and we tracked the nucleosynthetic yields for several elements: D, ^{4}He, C, N, O, Si, S, Fe, Zn as a function of redshift, both in the IGM and in the ISM of the growing structures. We compared the results of these models with the observed abundances in the Lyman α forest and in DLAs. We also considered possible constraints associated with the observations of the two extremely metal-poor stars HE 0107-5240 and CS22949-037. We have shown that a bimodal (or top-heavy) IMF (40 - 100 $M_\odot$) best satifies all constraints applied. In contrast, models with an extreme mass range ($\gtrsim 100\ M_\odot$) often assumed to be responsible for the early stages of reionization do less well.

As motivated by the numerical simulations of first star formation (Abel, Bryan, & Norman 2002; Bromm, Coppi, & Larson 2002), a mode of even more extreme stellar masses in the range ($\geq 270\ M_\odot$) has also been considered. As all massive stars collapse entirely into black holes in this mode, the chemical evolution and the reionization are de-correlated, as already mentioned by Tumlinson et al. (2004). The ionizing flux from these very massive stars can easily reionize the Universe at $z \sim 17$. However the chemical evolution in this case is exactly the same as in the standard star formation model, and the high redshift abundances are not reproduced. Consequently, the suggestion (Bromm & Loeb 2003) that such Population III stars were the precursors of the extreme metal-poor halo stars is untenable. There is no evidence, nor any need, for a hypothesised primordial population of very massive stars in order to account for the chemical abundances of extremely metal-poor halo stars or of the intergalactic medium. The combined population of early-forming, normal (0.1 - 100 $M_\odot$) and massive (40 - 100 $M_\odot$) stars can simultaneously explain the cosmic chemical evolution and the observations of extremely metal-poor halo stars and also account for early cosmological reionization.

We have shown that the initial massive starburst, which originally was introduced to reionize the early Universe, produces rapid initial metal pollution. The existence of old, C-rich halo stars with high [O/Fe] and [C/Fe] ratios is predicted as a consequence of these massive stars. The recently observed abundances in the oldest halo stars could trace this very specific stellar population.

We have also found that the D abundance is strongly coupled to the gas fraction in the structures, with the implication that local D measurements are a non-robust cosmological probe. In addition, there is some non-primordial contribution to the He abundance even in metal-poor galaxies, that is however within the observed range.

Our suggestion is far from the whole story. There must be late ionization input by harder photons than produced by OB stars to account for the He II abundance at $z \sim 2-4$, for example associated with the quasar population (Hui & Haiman 2003) or Pop III stars (Bromm, Kudritzki, & Loeb 2001b; Venkatesan, Tumlinson, & Shull 2003). As structure builds up, the ionizing photon escape fraction will surely decrease, and the intergalactic medium is likely to recombine before $z \sim 6$, at which time the neutral fraction is constrained from the onset of the Gunn-Peterson effect to be about 0.001%. Cen (2003b) has suggested that the Universe becomes neutral again at $z \sim 13$ and is reionized for the second time at $z \sim 6$, not necessary by the same stellar population. However our calculations suggests that normal star formation is likely to suffice at this epoch (Gnedin 2004) in order to account for the observed ionization level.

The authors warmly thank Roger Cayrel and Patrick Petitjean for frequent fruitful discussions. This work was supported in part by DOE grants DE-FG02-94ER-40823 at the University of Minnesota, and by PICS 1076 CNRS France/USA.

REFERENCES

Abel, T., Bryan, G. L., & Norman, M. L. 2002, Science, 295, 93

Aguirre, A., Schaye, J., Kim, T., Theuns, T., Rauch, M., & Sargent, W. L. W. 2004, ApJ, 602, 38

Ashenfelter, T., Mathews, G. J., & Olive, K. A. 2004a, Phys. Rev. Lett., 92, 041102

Ashenfelter, T. P., Mathews, G. J., & Olive, K. A. 2004b, astro-ph/0404257

Becker, R. H., Fan, X., White, R. L., Strauss, M. A., Narayanan, V. K., Lupton, R. H., Gunn, J. E., Annis, J., Bahcall, N. A., Brinkmann, J., Connolly, A. J., Csabai, I., Czarapata, P. C., Doi, M., Heckman, T. M., Hennessy, G. S., Ivezić, Ž., Knapp, G. R., Lamb, D. Q., McKay, T. A., Munn, J. A., Nash, T., Nichol, R., Pier, J. R., Richards, G. T., Schneider, D. P., Stoughton, C., Szalay, A. S., Thakar, A. R., & York, D. G. 2001, AJ, 122, 2850

Bessell, M. S., Christlieb, N., & Gustafsson, B. 2004, astro-ph/0401450

Bihain, G., Israelian, G., Rebolo, R., Bonifacio, P., & Molaro, P. 2004, astro-ph/0405050

Bromm, V. 2004, PASP, 116, 103

Bromm, V., Coppi, P. S., & Larson, R. B. 2002, ApJ, 564, 23

Bromm, V., Ferrara, A., Coppi, P. S., & Larson, R. B. 2001a, MNRAS, 328, 969

Bromm, V., Kudritzki, R. P., & Loeb, A. 2001b, ApJ, 552, 464

Bromm, V. & Loeb, A. 2003, Nature, 425, 812

Burles, S. & Tytler, D. 1998a, ApJ, 499, 699

—. 1998b, ApJ, 507, 732

Cassé, M., Olive, K. A., Vangioni-Flam, E., & Audouze, J. 1998, New A, 3, 259

Cen, R. 2003a, ApJ, 591, L5

—. 2003b, ApJ, 591, 12

Centurión, M., Molaro, P., Vladilo, G., Péroux, C., Levshakov, S. A., & D'Odorico, V. 2003, A&A, 403, 55

Chand, H., Srianand, R., Petitjean, P., & Aracil, B. 2004, astro-ph/0401094

Christlieb, N., Gustafsson, B., Korn, A. J., Barklem, P. S., Beers, T. C., Bessell, M. S., Karlsson, T., & Mizuno-Wiedner, M. 2004, ApJ, 603, 708

Ciardi, B., Ferrara, A., & White, S. D. M. 2003, MNRAS, 344, L7

Coc, A., Vangioni-Flam, E., Descouvemont, P., Adahchour, A., & Angulo, C. 2004, ApJ, 600, 544

Crighton, N. H. M., Webb, J. K., Ortiz-Gil, A., & Fernandez-Soto, A. 2004, astro-ph/0403512

Cyburt, R. H., Fields, B. D., & Olive, K. A. 2003, Physics Letters B, 567, 227

Depagne, E., Hill, V., Spite, M., Spite, F., Plez, B., Beers, T. C., Barbuy, B., Cayrel, R., Andersen, J., Bonifacio, P., François, P., Nordström, B., & Primas, F. 2002, A&A, 390, 187

Dickinson, M., Papovich, C., Ferguson, H. C., & Budavári, T. 2003, ApJ, 587, 25

Dijkstra, M., Haiman, Z., & Loeb, A. 2004a, astro-ph/0403078

Dijkstra, M., Haiman, Z., Rees, M. J., & Weinberg, D. H. 2004b, ApJ, 601, 666

Fields, B. D., Olive, K. A., Silk, J., Cassé, M., & Vangioni-Flam, E. 2001, ApJ, 563, 653

Fukugita, M., Hogan, C. J., & Peebles, P. J. E. 1998, ApJ, 503, 518

Giavalisco, M., Dickinson, M., Ferguson, H. C., Ravindranath, S., Kretchmer, C., Moustakas, L. A., Madau, P., Fall, S. M., Gardner, J. P., Livio, M., Papovich, C., Renzini, A., Spinrad, H., Stern, D., & Riess, A. 2004, ApJ, 600, L103

Gnedin, N. Y. 2004, astro-ph/0403699

Hébrard, G. & Moos, H. W. 2003, ApJ, 599, 297

Haiman, Z. & Holder, G. P. 2003, ApJ, 595, 1

Heger, A., Fryer, C. L., Woosley, S. E., Langer, N., & Hartmann, D. H. 2003, ApJ, 591, 288

Heger, A. & Woosley, S. E. 2002, ApJ, 567, 532

Hui, L. & Haiman, Z. 2003, ApJ, 596, 9

Israelian, G., Shchukina, N., Rebolo, R., Basri, G., Gonzalez-Hernandez, J. I., & Kajino, T. 2004, astro-ph/0403033

Iwata, I., Ohta, K., Tamura, N., Ando, M., Wada, S., Watanabe, C., Akiyama, M., & Aoki, K. 2003, PASJ, 55, 415

Kirkman, D., Tytler, D., Suzuki, N., O'Meara, J. M., & Lubin, D. 2003, ApJS, 149, 1

Kogut, A., Spergel, D. N., Barnes, C., Bennett, C. L., Halpern, M., Hinshaw, G., Jarosik, N., Limon, M., Meyer, S. S., Page, L., Tucker, G. S., Wollack, E., & Wright, E. L. 2003, ApJS, 148, 161

Lanzetta, K. M., Yahata, N., Pascarelle, S., Chen, H., & Fernández-Soto, A. 2002, ApJ, 570, 492

Larson, R. B. 1986, MNRAS, 218, 409

Ledoux, C., Petitjean, P., & Srianand, R. 2003, MNRAS, 346, 209

Lilly, S. J., Le Fevre, O., Hammer, F., & Crampton, D. 1996, ApJ, 460, L1

Maeder, A. & Meynet, G. 1989, A&A, 210, 155

Mo, H. J. & White, S. D. M. 2002, MNRAS, 336, 112

Murphy, M. T., Webb, J. K., & Flambaum, V. V. 2003, MNRAS, 345, 609

Nagamine, K., Cen, R., Hernquist, L., Ostriker, J. P., & Springel, V. 2003, astro-ph/0311294

Oh, S. P. 2002, MNRAS, 336, 1021

Oh, S. P. & Haiman, Z. 2003, MNRAS, 346, 456

Oh, S. P., Nollett, K. M., Madau, P., & Wasserburg, G. J. 2001, ApJ, 562, L1

Olive, K. A., Thielemann, F., & Truran, J. W. 1987, ApJ, 313, 813

O'Meara, J. M., Tytler, D., Kirkman, D., Suzuki, N., Prochaska, J. X., Lubin, D., & Wolfe, A. M. 2001, ApJ, 552, 718

Ouchi, M., Shimasaku, K., Furusawa, H., Miyazaki, M., Doi, M., Hamabe, M., Hayashino, T., Kimura, M., Kodaira, K., Komiyama, Y., Matsuda, Y., Miyazaki, S., Nakata, F., Okamura, S., Sekiguchi, M., Shioya, Y., Tamura, H., Taniguchi, Y., Yagi, M., & Yasuda, N. 2003, ApJ, 582, 60

Pascarelle, S. M., Lanzetta, K. M., & Fernández-Soto, A. 1998, ApJ, 508, L1

Pelló, R., Schaerer, D., Richard, J., Le Borgne, J.-F., & Kneib, J.-P. 2004, A&A, 416, L35

Pettini, M. 2003, astro-ph/0303272

Pettini, M. & Bowen, D. V. 2001, ApJ, 560, 41

Pettini, M., Ellison, S. L., Bergeron, J., & Petitjean, P. 2002, A&A, 391, 21

Prochaska, J. X., Gawiser, E., Wolfe, A. M., Castro, S., & Djorgovski, S. G. 2003, ApJ, 595, L9

Qian, Y.-Z. & Wasserburg, G. J. 2001, ApJ, 559, 925

Ricotti, M. 2002, MNRAS, 336, L33

Ricotti, M., Haehnelt, M. G., Pettini, M., & Rees, M. J. 2004, astro-ph/0403327

Ricotti, M. & Ostriker, J. P. 2004, MNRAS, 350, 539

Scalo, J. M. 1986, Fund. Cosmic Phys., 11, 1

Schaerer, D. 2002, A&A, 382, 28

Schaye, J., Aguirre, A., Kim, T., Theuns, T., Rauch, M., & Sargent, W. L. W. 2003, ApJ, 596, 768

Schneider, R., Ferrara, A., Natarajan, P., & Omukai, K. 2002, ApJ, 571, 30

Scully, S., Casse, M., Olive, K. A., & Vangioni-Flam, E. 1997, ApJ, 476, 521

Sembach, K. R., Wakker, B. P., Tripp, T. M., Richter, P., Kruk, J. W., Blair, W. P., Moos, H. W., Savage, B. D., Shull, J. M., York, D. G., Sonneborn, G., Hébrard, G., Ferlet, R., Vidal-Madjar, A., Friedman, S. D., & Jenkins, E. B. 2004, ApJS, 150, 387

Shapley, A. E., Erb, D. K., Pettini, M., Steidel, C. C., & Adelberger, K. L. 2004, astro-ph/0405187

Simcoe, R. A., Sargent, W. L. W., & Rauch, M. 2004, ApJ, 606, 92

Songaila, A. 2001, ApJ, 561, L153

Spergel, D. N., Verde, L., Peiris, H. V., Komatsu, E., Nolta, M. R., Bennett, C. L., Halpern, M., Hinshaw, G., Jarosik, N., Kogut, A., Limon, M., Meyer, S. S., Page, L., Tucker, G. S., Weiland, J. L., Wollack, E., & Wright, E. L. 2003, ApJS, 148, 175

Steidel, C. C., Pettini, M., & Adelberger, K. L. 2001, ApJ, 546, 665

Suda, T., Aikawa, M., Machida, M. N., Fujimoto, M. Y., & Iben Jr, I. 2004, astro-ph/0402589

Tinsley, B. M. 1980, Fund. Cosmic Phys., 5, 287

Truran, J. W. & Cameron, A. G. W. 1971, Ap&SS, 14, 179

Tumlinson, J., Venkatesan, A., & Shull, J. M. 2004, astro-ph/0401376

Umeda, H. & Nomoto, K. 2003, Nature, 422, 871

Vader, J. P. 1986, ApJ, 305, 669

van den Hoek, L. B. & Groenewegen, M. A. T. 1997, A&AS, 123, 305

Venkatesan, A., Schneider, R., & Ferrara, A. 2004, MNRAS, 349, L43

Venkatesan, A. & Truran, J. W. 2003, ApJ, 594, L1

Venkatesan, A., Tumlinson, J., & Shull, J. M. 2003, ApJ, 584, 621

Wasserburg, G. J. & Qian, Y.-Z. 2000, ApJ, 538, L99

Woosley, S. E. & Weaver, T. A. 1995, ApJS, 101, 181

Wyithe, J. S. B. & Loeb, A. 2003, ApJ, 588, L69

Zentner, A. R. & Bullock, J. S. 2003, ApJ, 598, 49

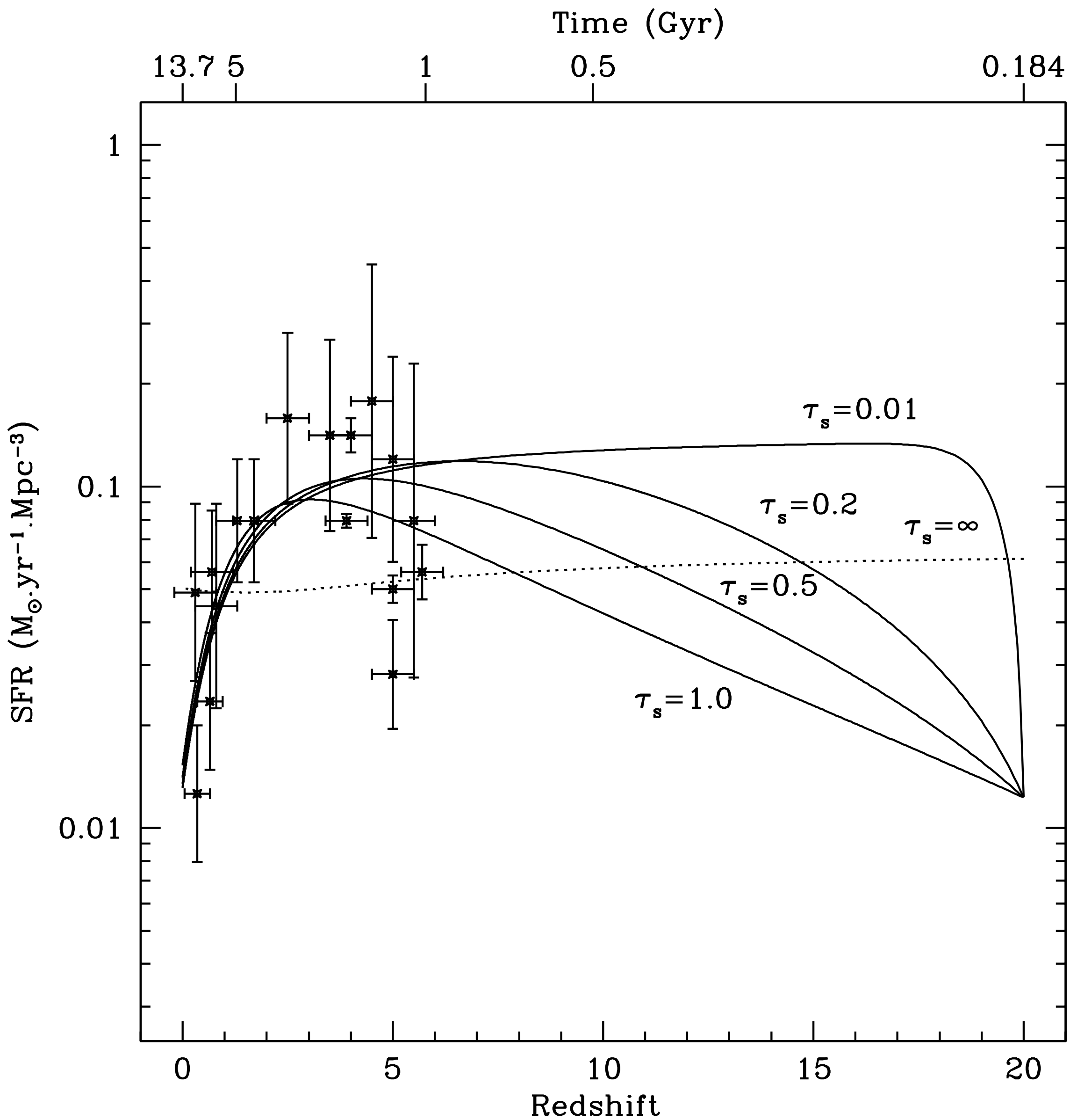

Fig. 1.— **Cosmic star formation rate : standard model (Model 0).** The observed cosmic SFR is taken from Lilly et al. (1996), Pascarelle et al. (1998), Iwata et al. (2003), Ouchi et al. (2003) and Giavalisco et al. (2004). We consider two possible scenarios for structure formation : either a uniform baryon accretion rate from $z = 20$ to $z = 0$ (dotted line) or an exponentially decreasing accretion rate (solid line) with a timescale τ_s as labelled.

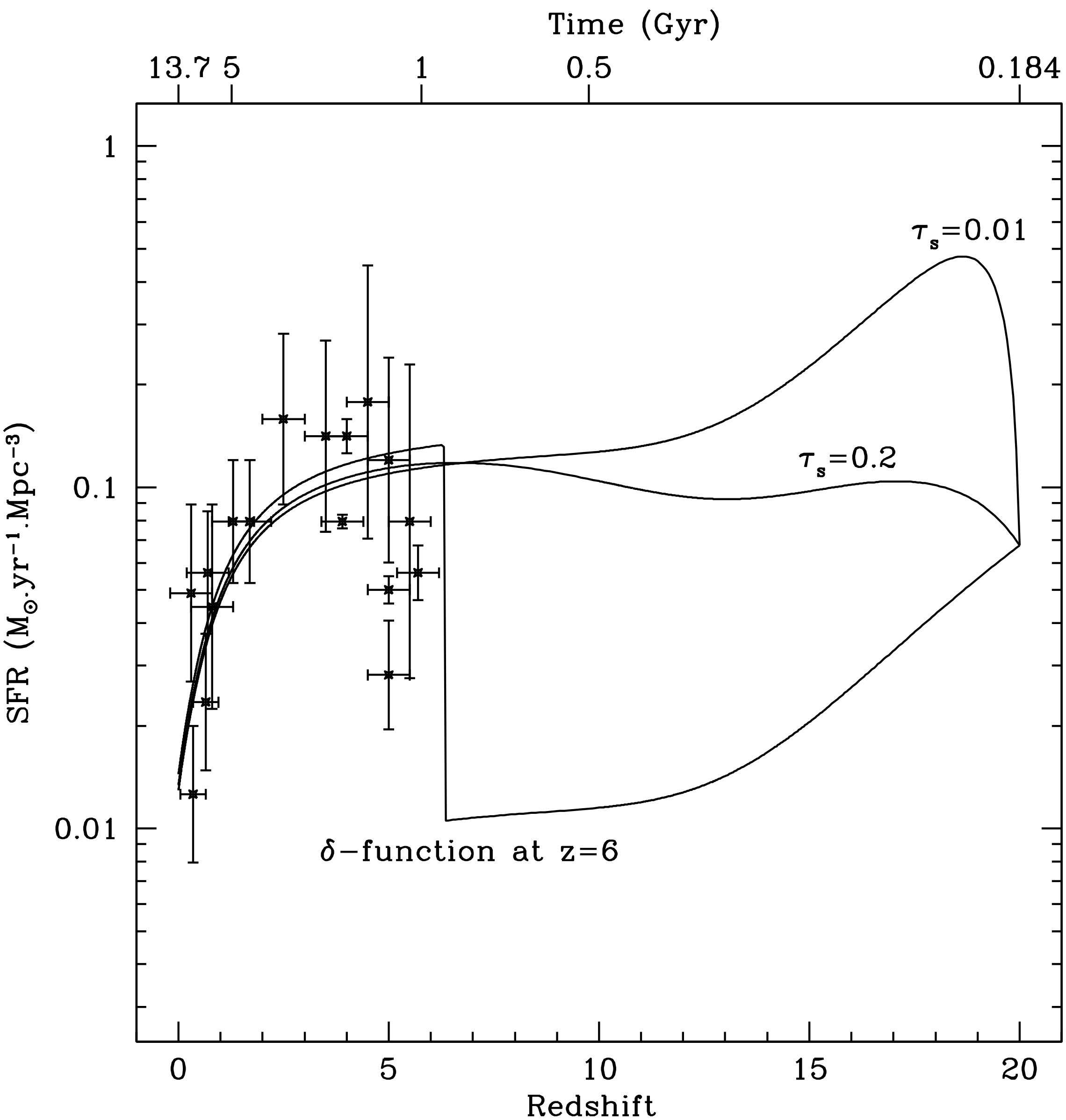

Fig. 2.— **Cosmic star formation rate : standard model + massive mode (Model 1).** Same as in figure 1. The two envisaged scenarios for structure formation are now either an exponentially decreasing accretion rate with timescale τ_s or a late impulse of structure formation at $z = 6$.

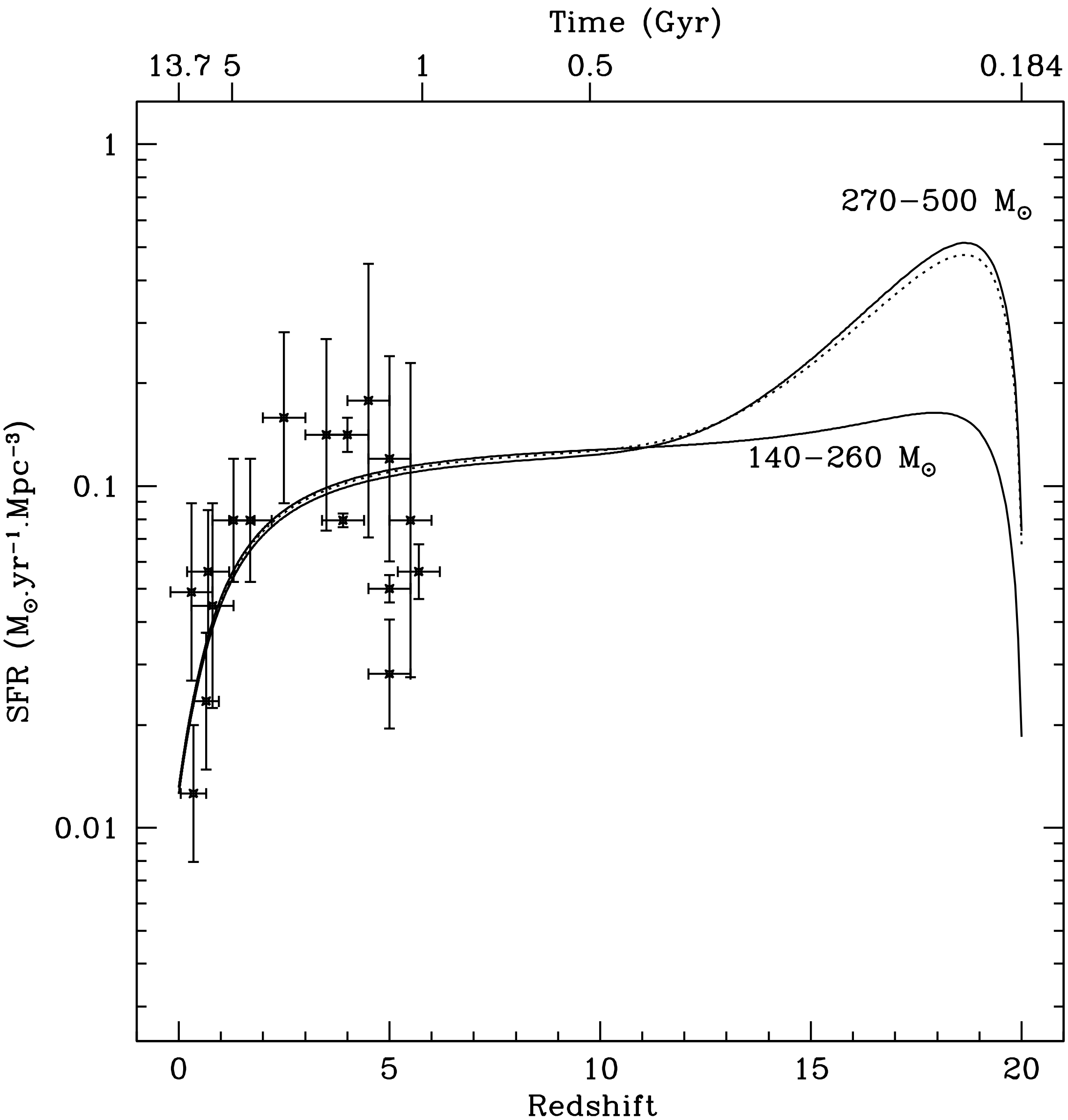

Fig. 3.— **Cosmic star formation rate : standard model + very massive mode (Models 2a and 2b).** Same as in figure 1. Models 2a and 2b are labeled with their mass range. Model 1 with $\tau_s = 0.01$ has been plotted (dotted line) for comparison.

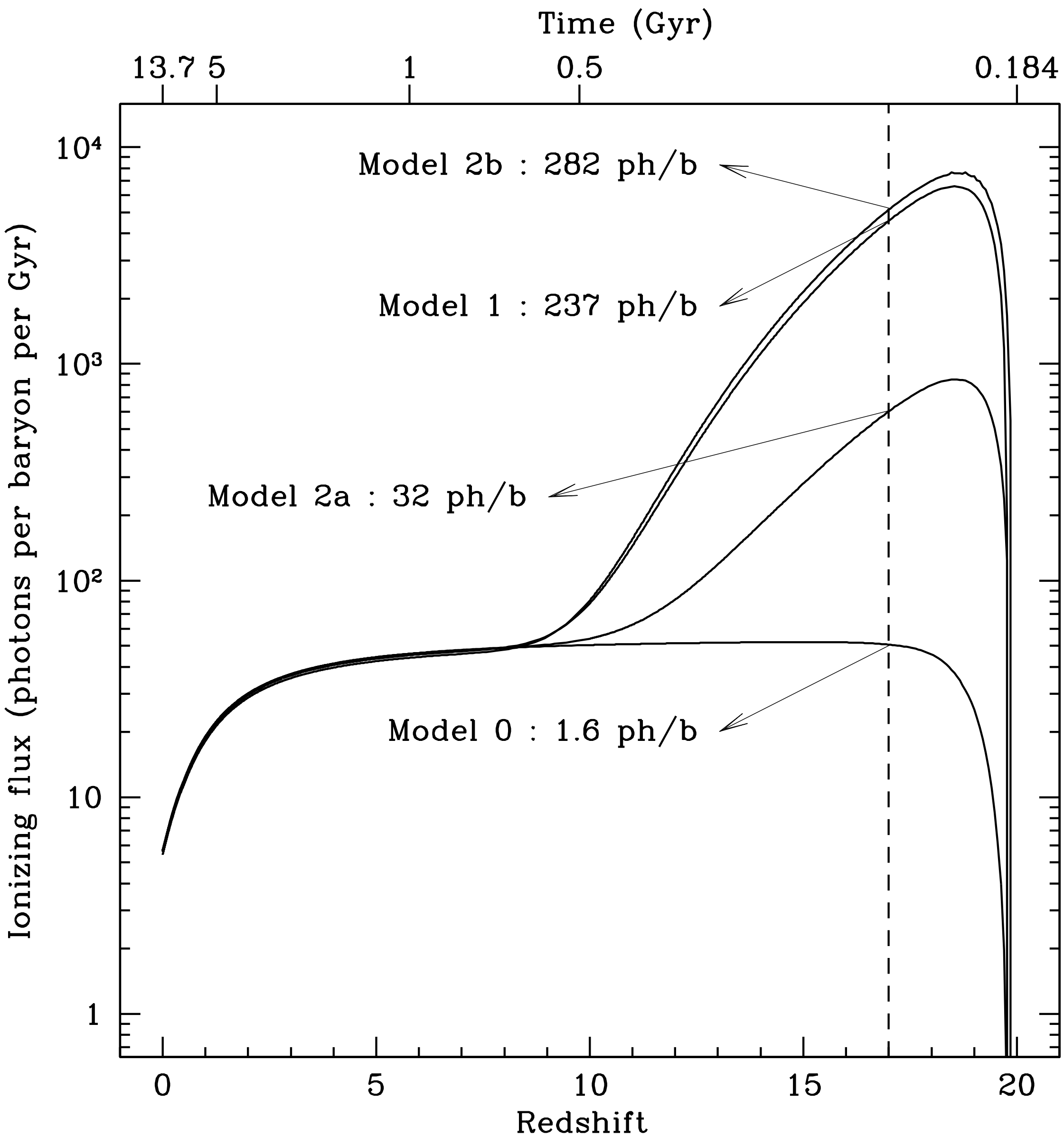

Fig. 4.— **Reionization.** The ionizing flux is plotted as function of redshift for the four models considered (0, 1, 2a and 2b). The total number of ionizing photons per intergalactic baryon produced at $z = 17$ is labeled for each curve. Only a fraction $f_{\rm esc}$ of these photons are available for the early reionization of the Universe, which is possible above ~ 10 photons per intergalactic baryon (see Figure 5).

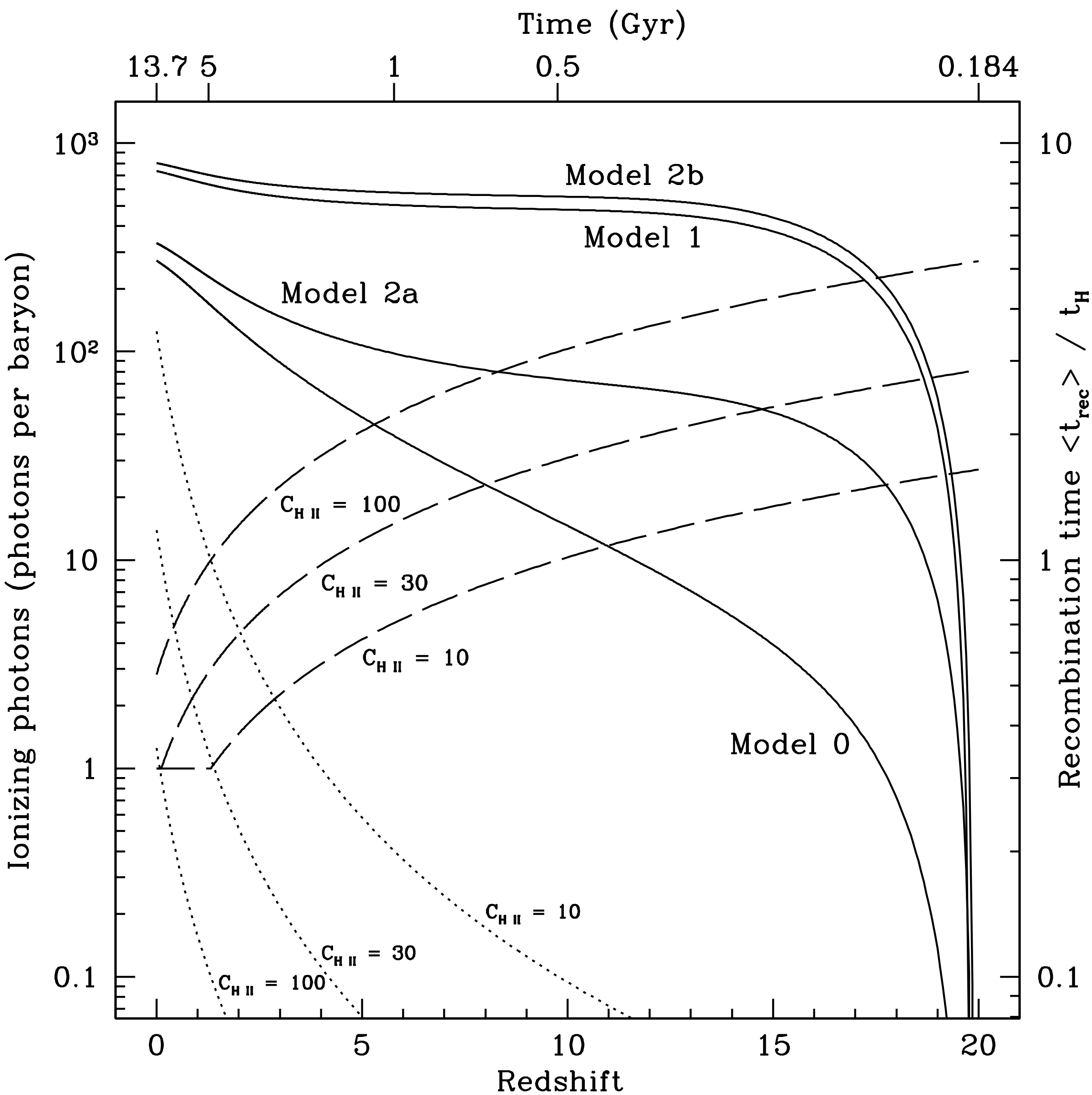

Fig. 5.— **Reionization.** The total number of ionizing photons per intergalactic baryon is plotted as function of redshift for the four models considered (solid lines : 0, 1, 2a and 2b). Only a fraction $f_{\rm esc}$ of these photons are available to reionize the IGM. The full reionization of the IGM is possible at redshift z if the number of UV photons per intergalactic baryon produced by stars has reached a minimum value which is plotted by the dashed lines. The minimum number is computed from the mean recombination time of an atom ionized at redshift z, and is plotted by the dotted lines in units of the Hubble time. Three values of the clumpiness factor of the ionized regions have been considered and are labeled in the figure : $C_{\rm H\,II} = 10$, 30 and 100.

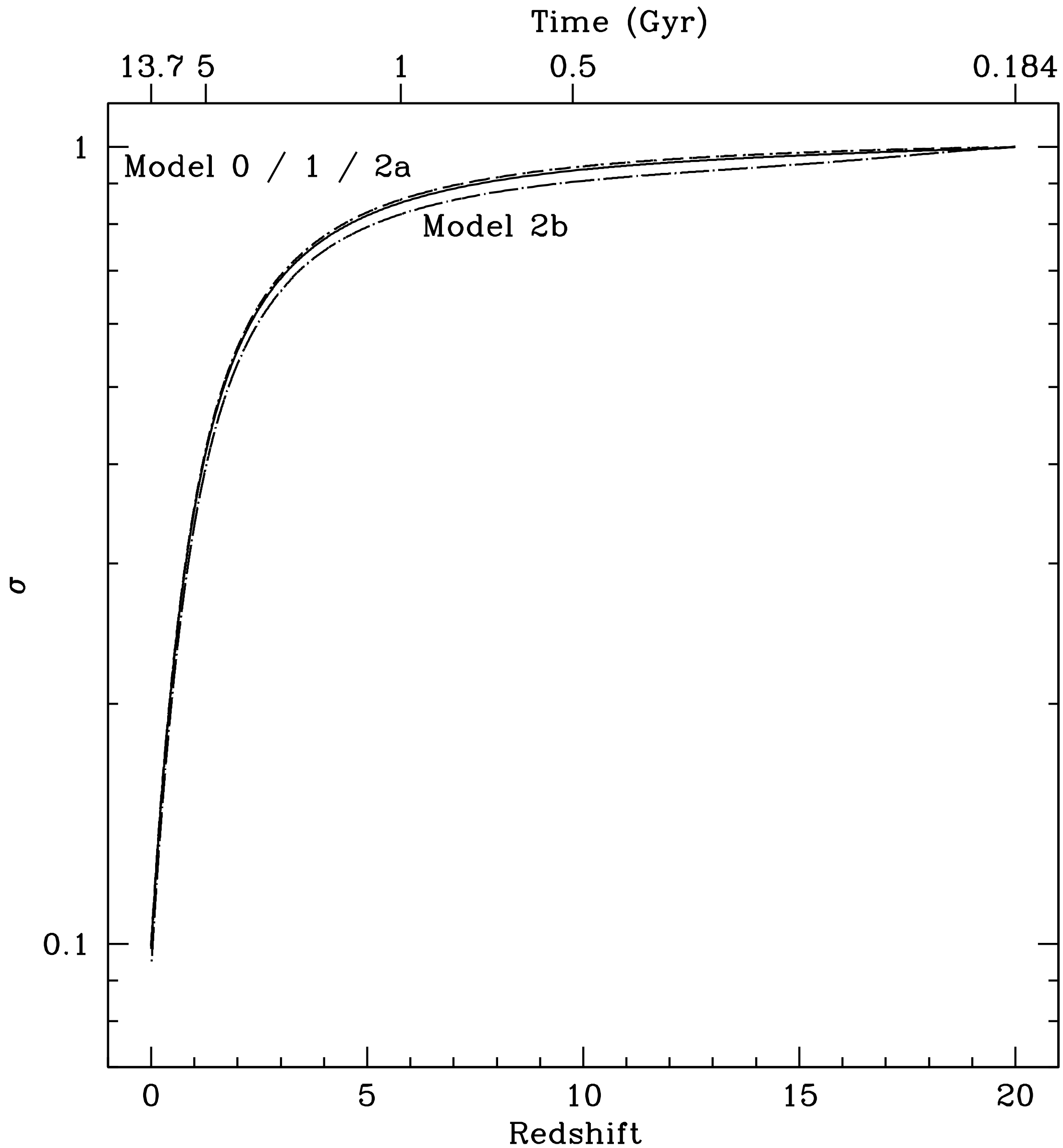

Fig. 6.— **Evolution of the gas fraction in the cosmic structures.** The gas mass fraction, σ, is plotted as a function of redshift for Model 0 (dotted line), Model 1 (solid line), Model 2a (dashed line) and Model 2b (dot-dashed line). Note that Models 0 and 2a are indistinguishable on this plot.

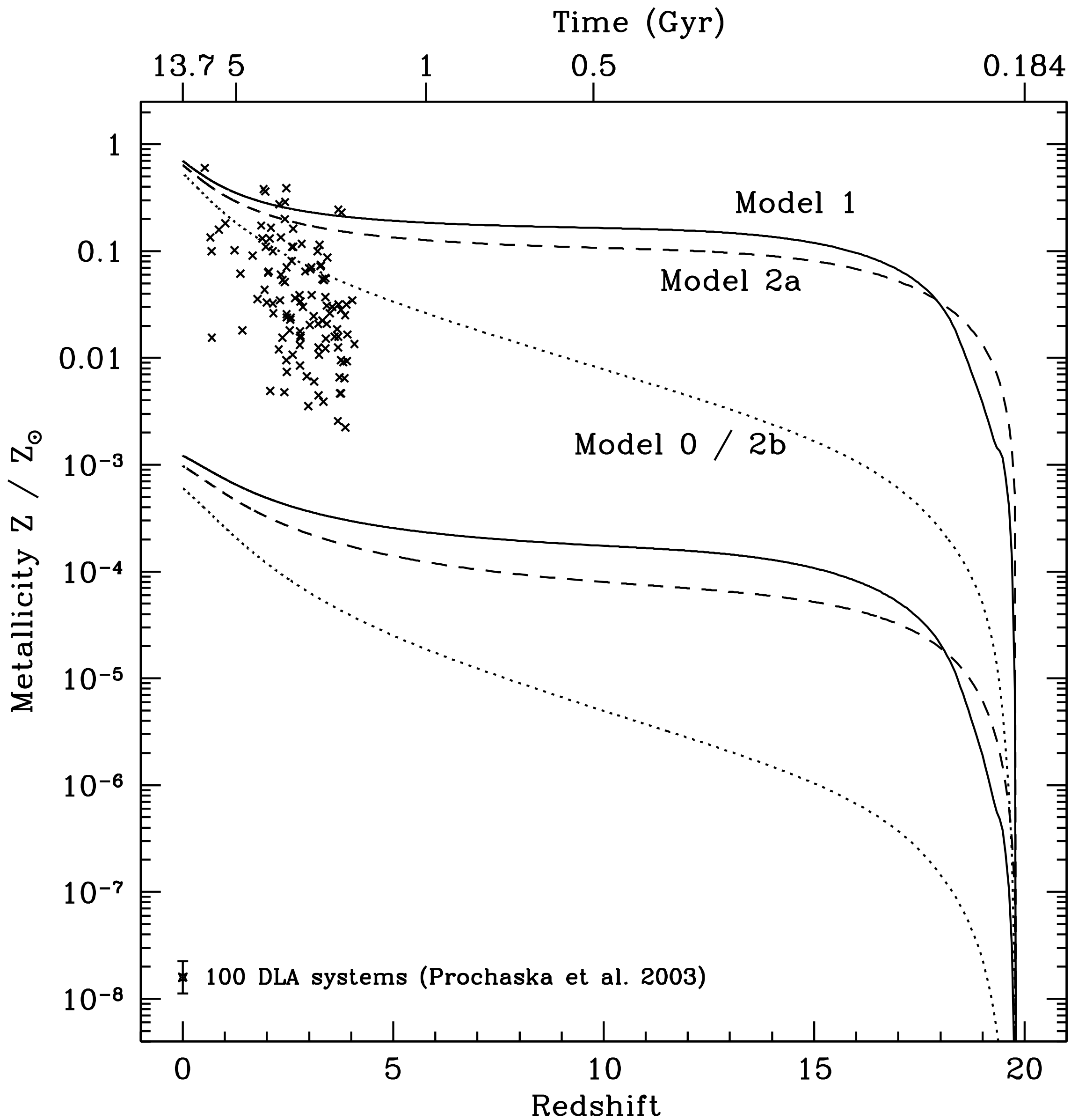

Fig. 7.— **Evolution of the global metallicity.** The metallicity in units of the solar metallicity is plotted as a function of redshift for three models : Model 0 (dotted line), Model 1 (solid line) and Model 2a (dashed line) both in the ISM of the cosmic structures (upper curves) and in the IGM (lower curves). The predictions of Model 2b are exactly the same as in Model 0.

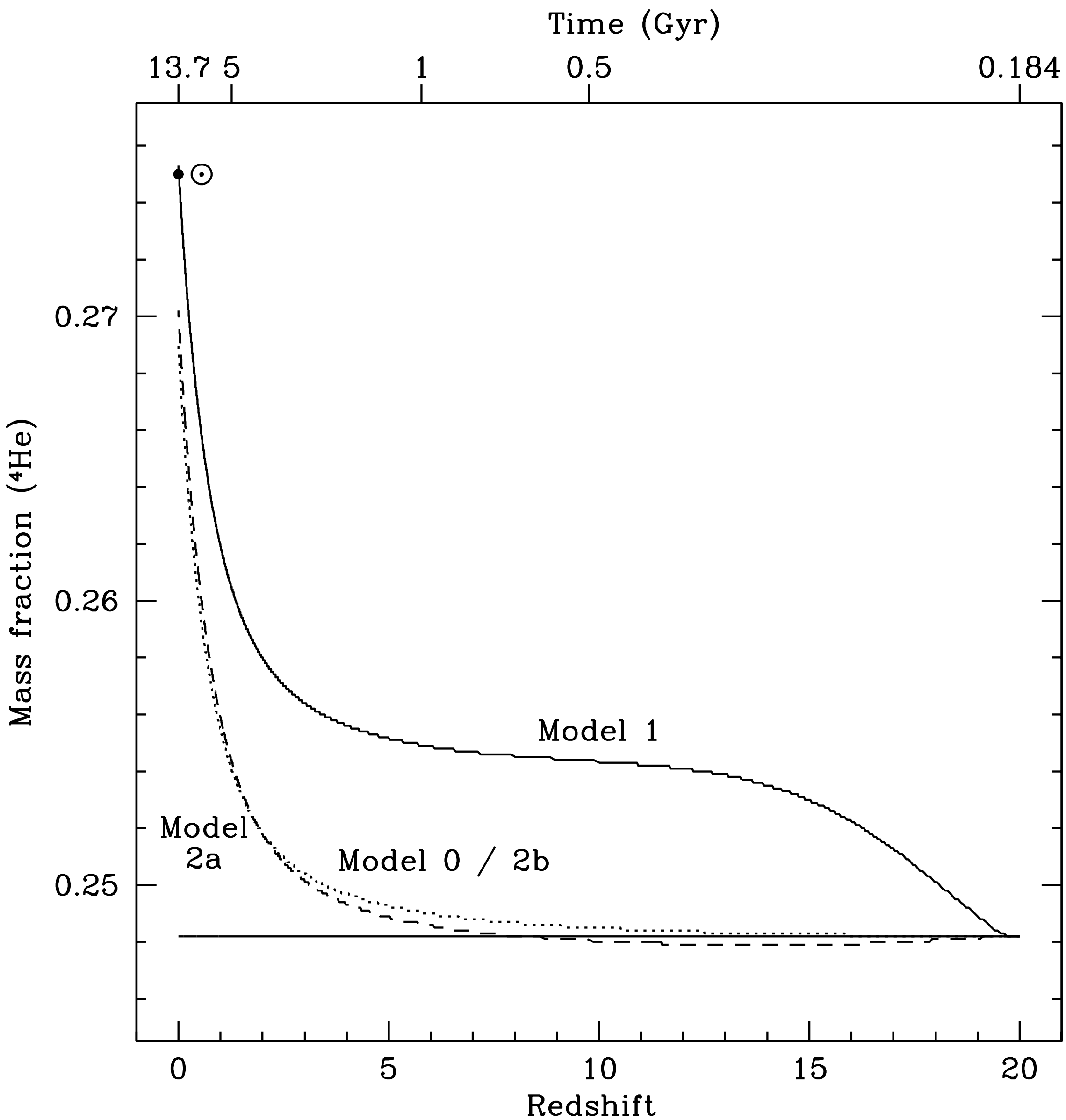

Fig. 8.— **Evolution of the Helium abundance.** The mass fraction of Helium in the cosmic structures is plotted as a function of redshift for Model 0 and 2b (dotted line), Model 1 (solid line) and Model 2a (dashed line). The BBN value is indicated as a horizontal solid line, which in all models also corresponds to the value in the IGM. The local abundance is indicated by the symbol ⊙.

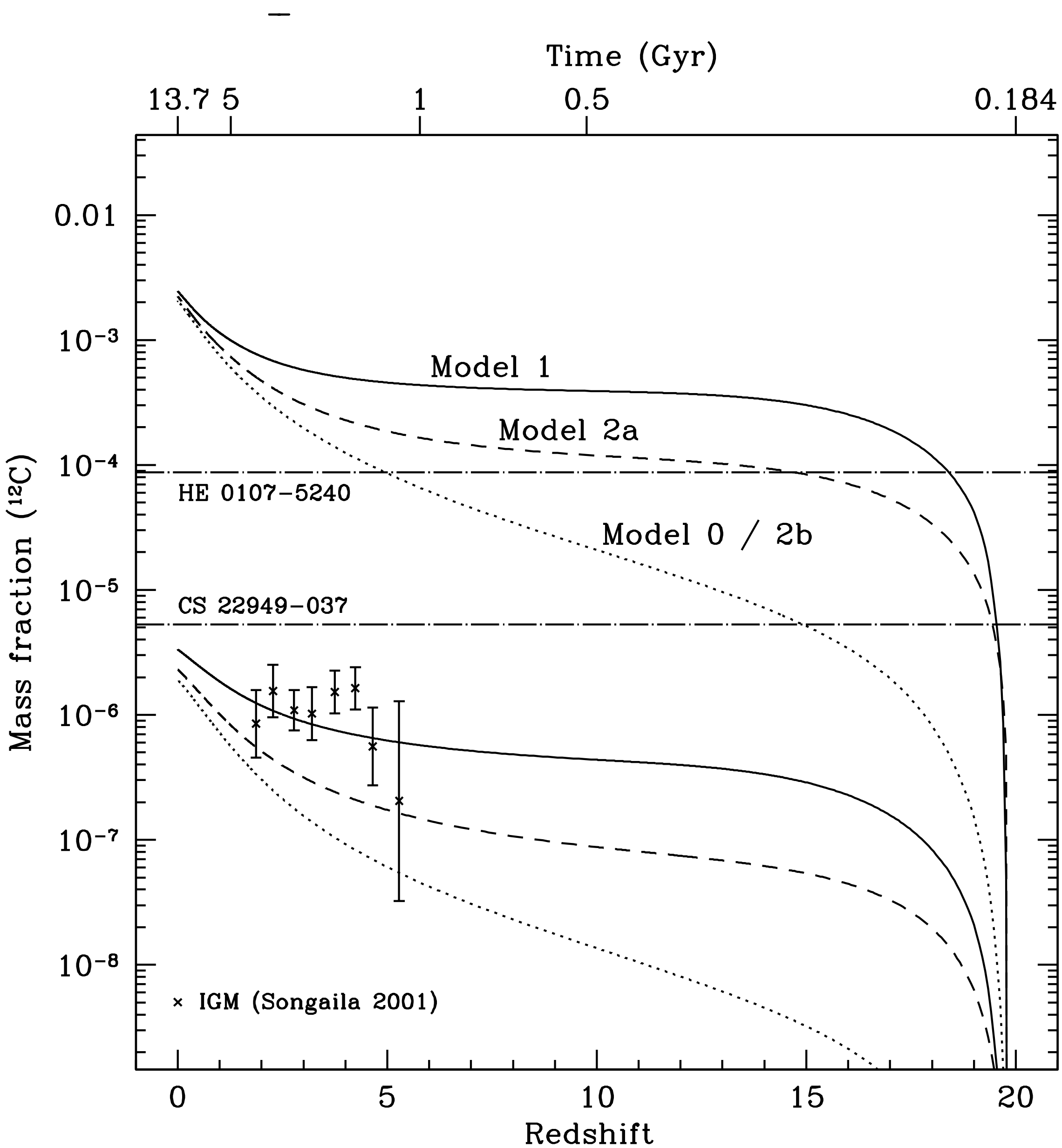

Fig. 9.— **Evolution of the Carbon abundance.** The Carbon mass fraction is plotted as a function of redshift for three models : Model 0 (dotted line), Model 1 (solid line) and Model 2a (dashed line) both in the ISM of the cosmic structures (upper curves) and in the IGM (lower curves). The predictions of Model 2b are exactly the same as in Model 0. Note that data from Songaila (2001) in the IGM represent the abundance of CIV, which is a lower limit of the total Carbon abundance.

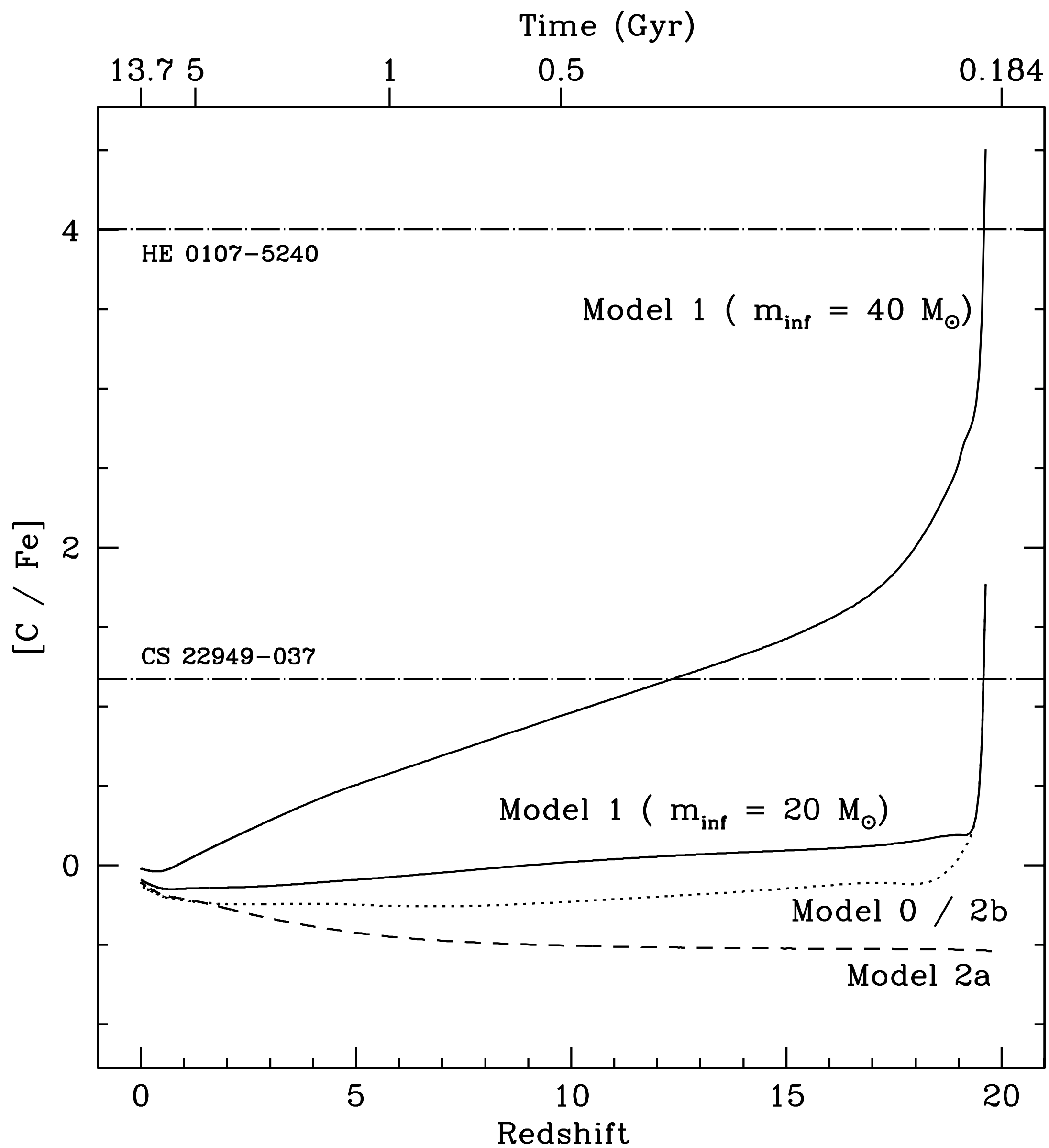

Fig. 10.— **Evolution of the [C/Fe] ratio.** This ratio in the cosmic structures is plotted as a function of redshift for Model 0 and 2b (dotted line), Model 1 (solid line) and Model 2a (dashed line). For Model 1, two lower mass limits of the IMF are considered : $m_{\rm inf} = 20$ M$_\odot$ or $m_{\rm inf} = 40$ M$_\odot$.

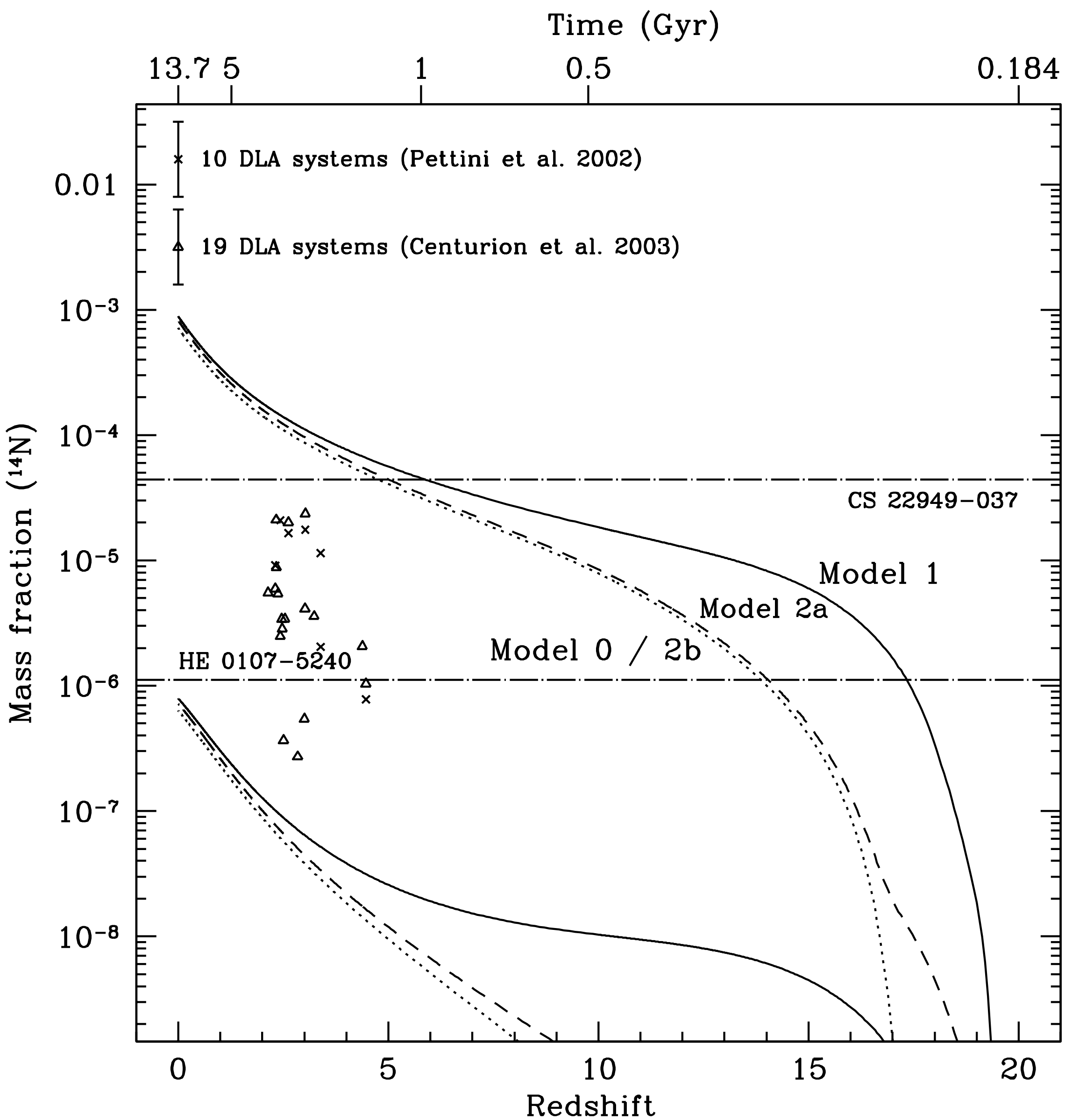

Fig. 11.— **Evolution of the Nitrogen abundance.** The Nitrogen mass fraction is plotted as a function of redshift as in Figure 9.

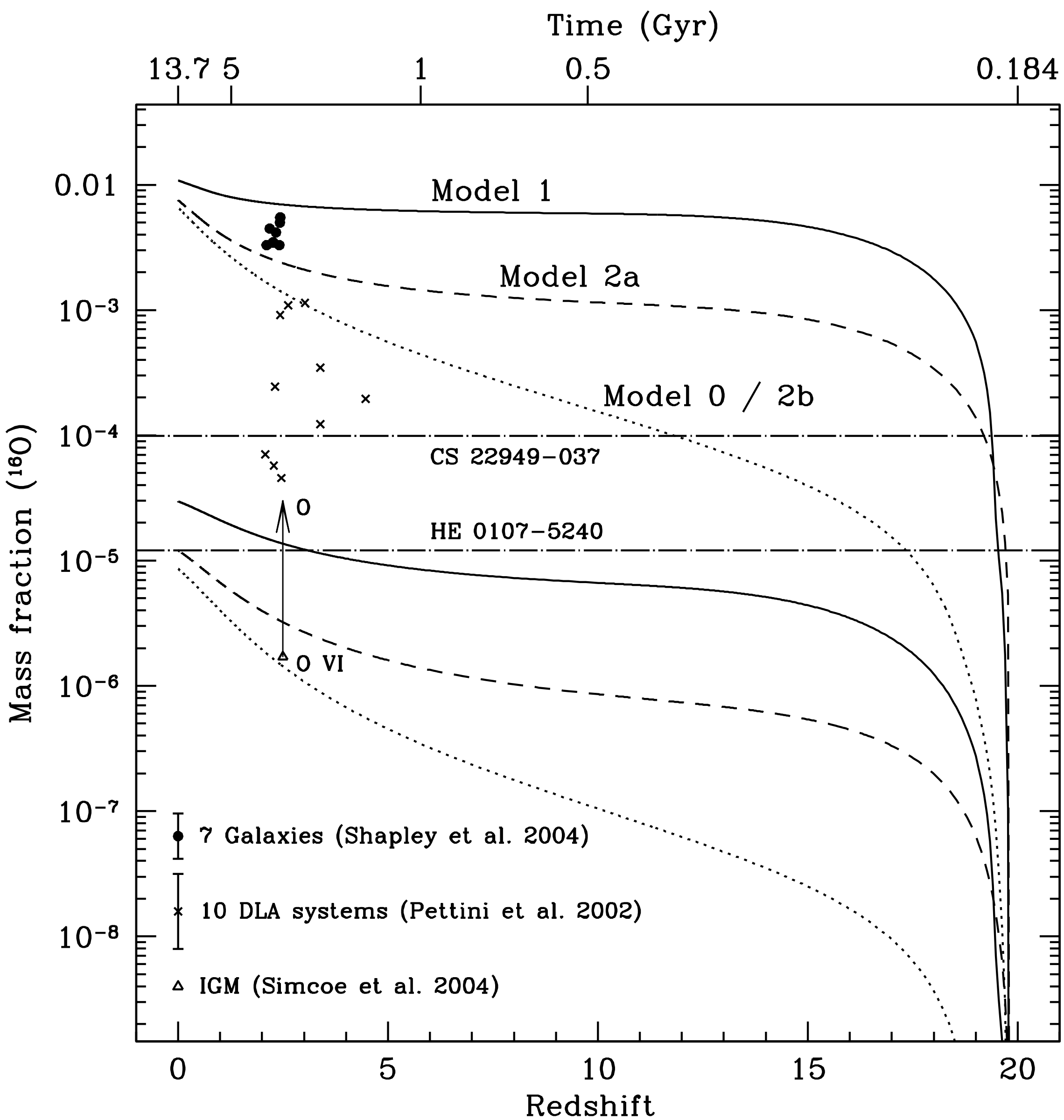

Fig. 12.— **Evolution of the Oxygen abundance.** The Oxygen mass fraction is plotted as a function of redshift as in Figure 9. Note that Simcoe et al. (2004) measure the abundance of O VI in the IGM. The arrow indicates the value of the Oxygen abundance they derive using ionization correction factors.

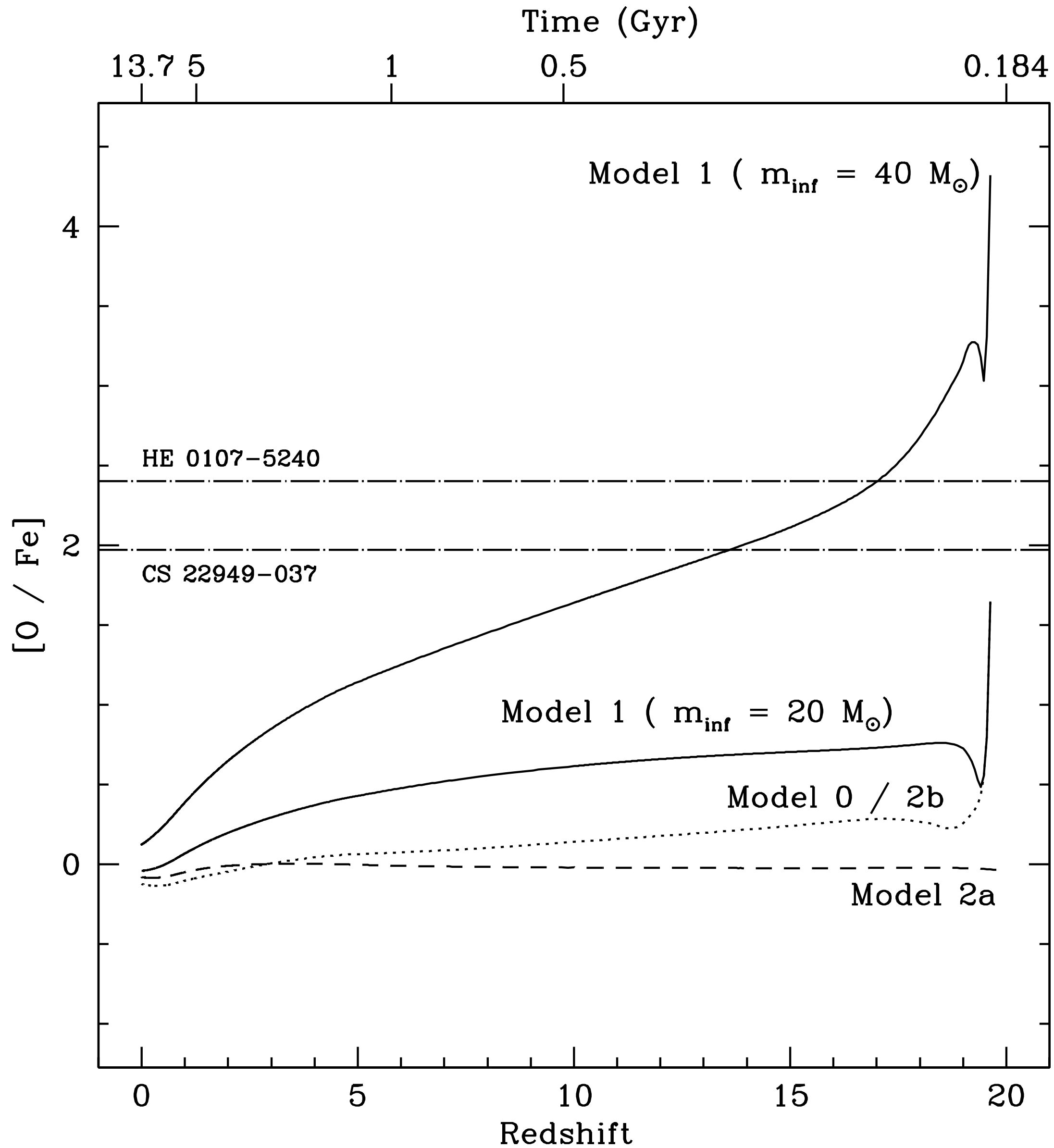

Fig. 13.— **Evolution of the [O/Fe] ratio.** The Oxygen to Iron ratio in the cosmic structures is plotted as a function of redshift for Model 0 and 2b (dotted line), Model 1 (solid line) and Model 2a (dashed line). For Model 1, two lower mass limits of the IMF are considered : $m_{\rm inf} = 20\ {\rm M}_{\odot}$ or $m_{\rm inf} = 40\ {\rm M}_{\odot}$.

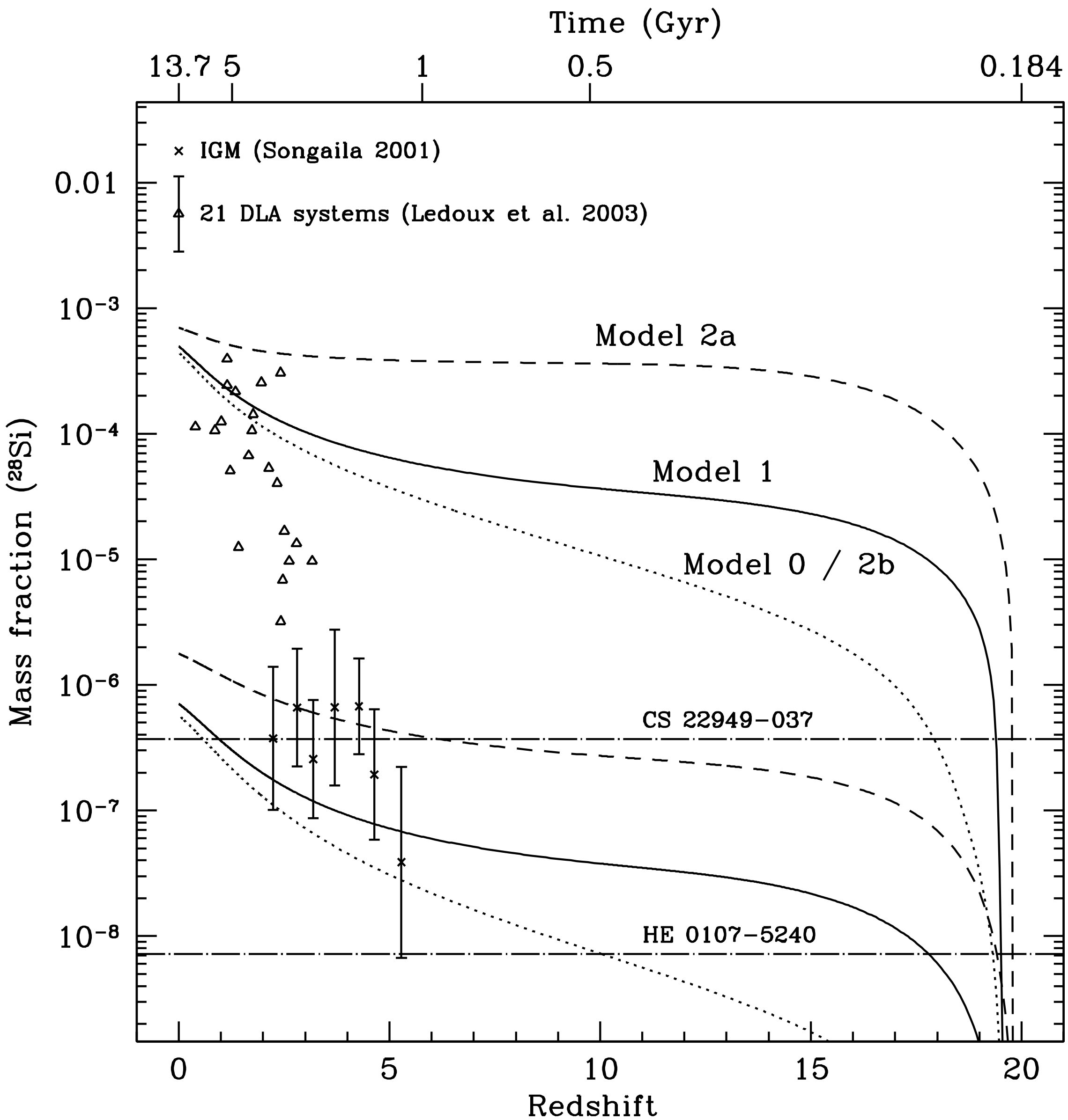

Fig. 14.— **Evolution of the Silicon abundance.** The Silicon mass fraction is plotted as a function of redshift as in Figure 9. Note that data from Songaila (2001) in the IGM represent the abundance of SiIV, which is a lower limit of the total Silicon abundance.

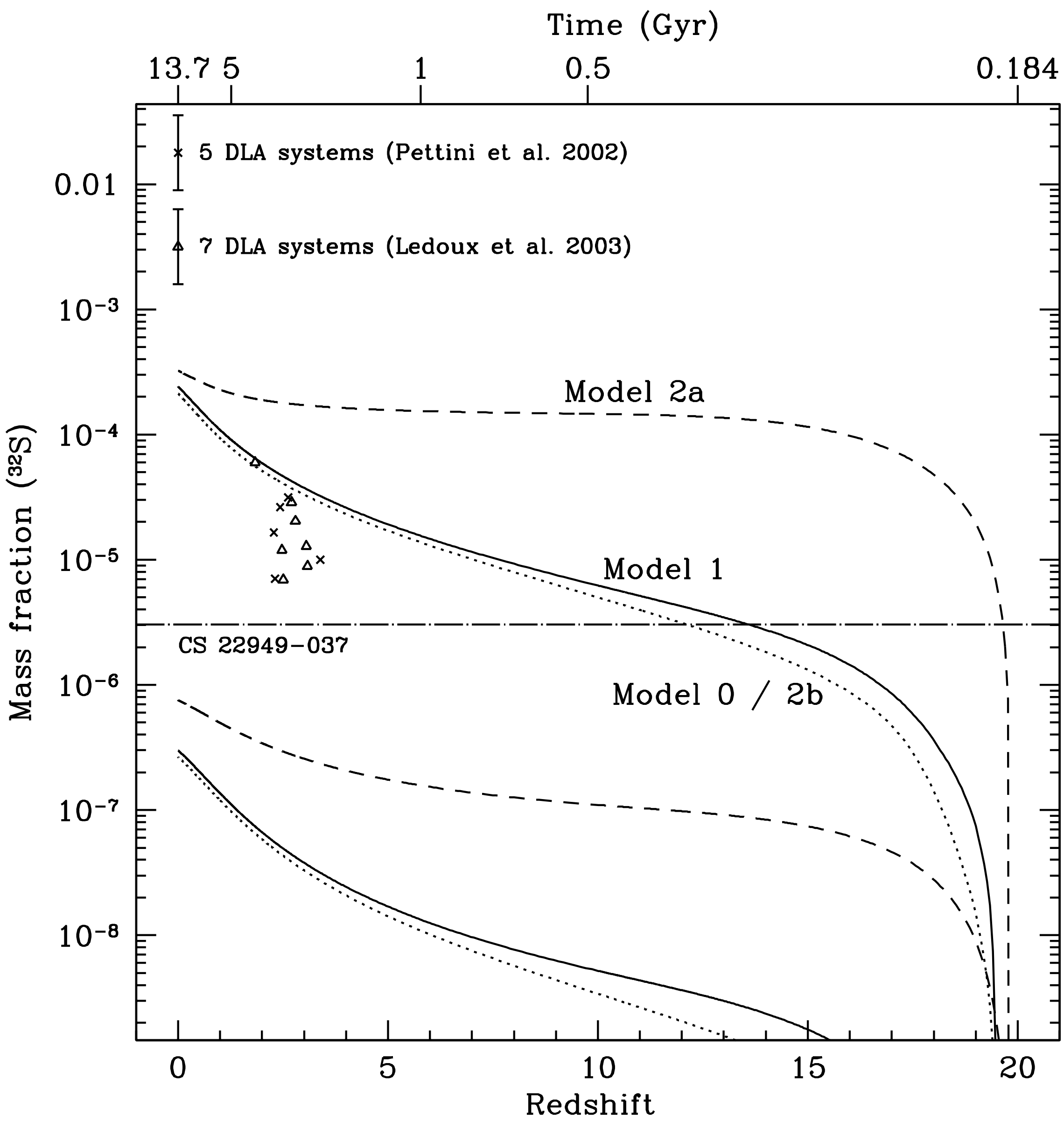

Fig. 15.— **Evolution of the Sulfur abundance.** The Sulpher mass fraction is plotted as a function of redshift as in Figure 9.

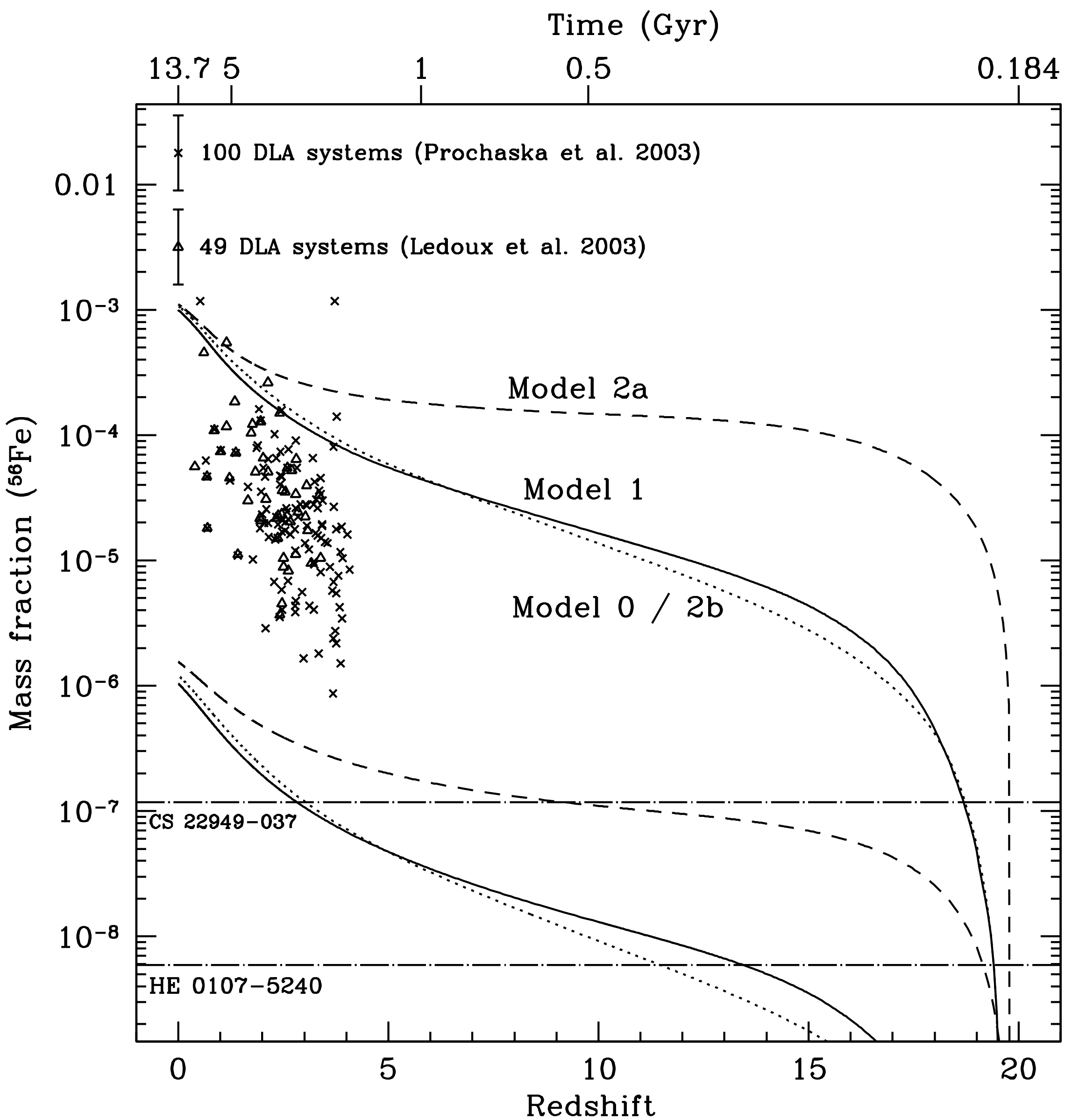

Fig. 16.— **Evolution of the Iron abundance.** The Iron mass fraction is plotted as a function of redshift as in Figure 9.

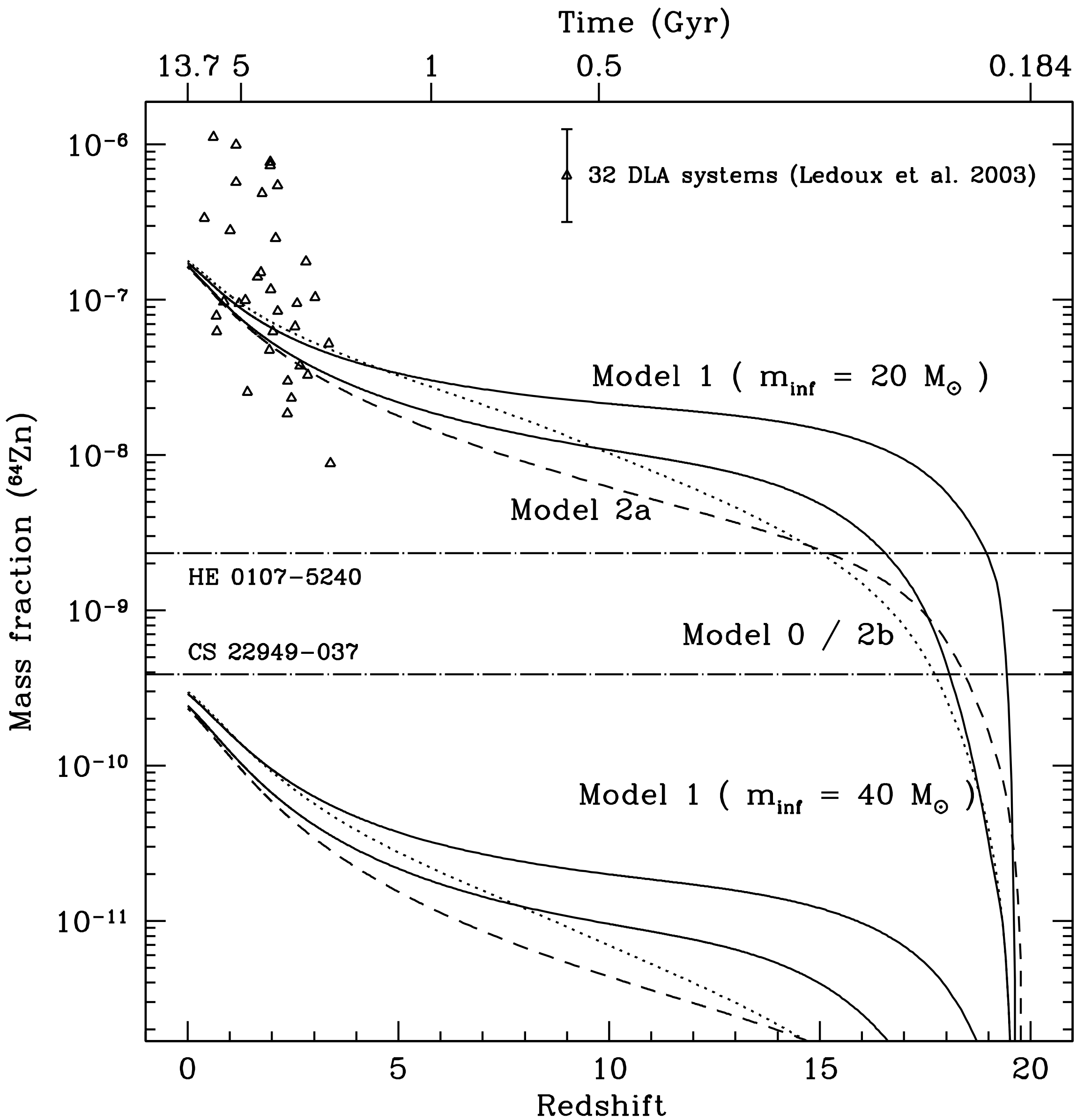

Fig. 17.— **Evolution of the Zinc abundance.** The Zinc mass fraction is plotted as a function of redshift as in Figure 9. For Model 1, two lower mass limits of the IMF are considered : $m_{\rm inf} = 20$ M$_\odot$ or $m_{\rm inf} = 40$ M$_\odot$.

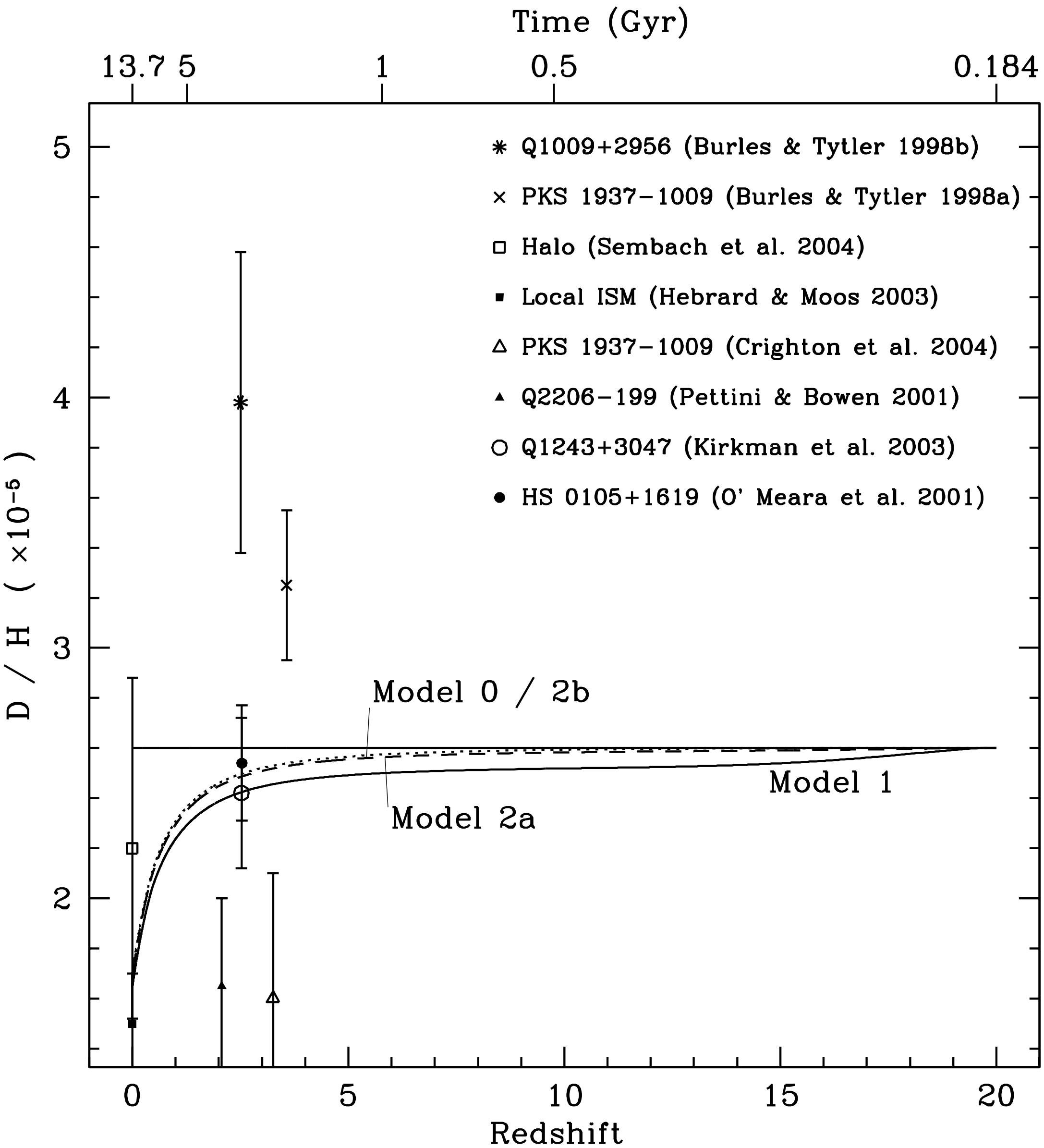

Fig. 18.— **Evolution of the Deuterium abundance.** The D/H ratio is plotted as a function of redshift in the ISM of the cosmic structures for Model 0 and 2b (dotted line), Model 1 (solid line) and Model 2a (dashed line). The BBN value is indicated as an horizontal solid line, which in all models also corresponds to the value in the IGM.